Construction of invariant compact finite-difference schemes

E. Ozbenli [*] and P. Vedula[†]

School of Aerospace and Mechanical Engineering, University of Oklahoma, 865 Asp Ave., Norman, Oklahoma 73019, USA

In this paper we propose a method, which is based on equivariant moving frames, for development of high-order accurate invariant compact finite-difference schemes that preserve Lie symmetries of underlying partial differential equations. In this method, variable transformations that are obtained from the extended symmetry groups of partial differential equations (PDEs) are used to transform independent and dependent variables and derivative terms of compact finite-difference schemes (constructed for these PDEs) such that the resulting schemes are invariant under the chosen symmetry groups. The unknown symmetry parameters that arise from the application of these transformations are determined through selection of convenient moving frames. In some cases, owing to selection of convenient moving frames, numerical representation of invariant (or symmetry-preserving) compact numerical schemes is found to be notably simpler than that of standard, noninvariant compact numerical schemes. Further, the accuracy of these invariant compact schemes can be arbitrarily set to a desired order by considering suitable compact finite-difference algorithms. Application of the proposed method is demonstrated through construction of invariant compact finite-difference schemes for some common linear and nonlinear PDEs (including the linear advection-diffusion equation in one or two dimensions, the inviscid Burgers' equation in one dimension, viscous Burgers' equation in one or two dimensions, spherical Burgers' equation in one dimension, and shallow water equations in two dimensions). Results obtained from our numerical simulations indicate that invariant compact finite-difference schemes not only inherit selected symmetry properties of underlying PDEs, but are also comparably more accurate than the standard, noninvariant base numerical schemes considered here.

I. INTRODUCTION

Compact finite differencing based on Padé approximants is a commonly used high-order numerical method that is well documented in the literature [1–10]. An important objective of this method is to achieve high-order accuracy with a relatively small number of stencil points by relating a weighted sum of functions (or dependent variables) to a weighted sum of derivatives, evaluated at grid points. Hence, numerical solutions based on compact schemes are found to have good, spectral-like resolutions, solutions that exponentially converge with increasing resolution, especially in the case of short waves [1]. In this regard, Hirsh [1] presented a detailed application of compact finite differencing which included development and application of fourth-order accurate compact schemes to three test problems, namely, viscous Burgers' equation, Howarth's retarded boundary layer flow, and the incompressible driven cavity problem. The author also provided a brief discussion of how to treat boundary conditions when developing compact finite-difference schemes, which could be problematic in some cases. In another work, Lele [2] extended the earlier works on compact finite differencing by presenting finite-difference schemes that provide a better representation of shorter length scales for use on problems with a range of spatial scales. In addition, the author provided a detailed discussion on how to obtain compact finite-difference schemes

of various orders (up to tenth order) and treat the relevant boundary conditions. In a more recent work, Shukla *et al.* [7] presented a family of high-order compact schemes that are built on nonuniform grids with spatial orders of accuracy ranging from fourth to 20th. These compact schemes are constructed such that they maintain high-order accuracy not only in the interior of a domain, but also at its boundaries. The authors demonstrated the application of these compact schemes to the linear wave equation and two-dimensional (2D) incompressible Navier-Stokes equations, and verified the achievement of high-order accuracy for these problems. They further showed (via comparisons with benchmark solutions for the 2D driven cavity flow, thermal convection in a square box, and flow past an impulsively started cylinder) that these high-order compact schemes are stable and produce highly accurate results on stretched grids with more points clustered at boundaries. Although compact finite differencing is an efficient method for construction of high-order accurate numerical schemes, these schemes often ignore geometric properties of underlying differential equations as the focus is usually on the accuracy when developing these schemes. Schemes that preserve certain geometric properties (such as energy, momentum, symplecticity, Hamiltonian, and Poisson structures of equations) are usually considered as geometric integrators. It is well documented in literature that geometric integrators, which account for certain geometric properties of underlying differential equations, are likely to perform better than standard schemes that ignore such properties [11–18].

---
[*]Corresponding author: ozbenli@ou.edu
[†]pvedula@ou.edu

Lie symmetry groups of differential equations are also geometric properties that could be preserved in numerical schemes. Numerous researchers have proposed methods for construction of numerical schemes that preserve symmetry groups of underlying differential equations [19–43]. Most of these works can be categorized into two major groups. In the first group [20–24], invariants of difference equations are determined through Lie's infinitesimal approach, and then a set of these invariants are used to construct invariant schemes that converge to the original differential equations in the continuous limit. In the other group [33–43], point transformations based on symmetry groups of differential equations are applied to some base (noninvariant) numerical schemes, and the unknown symmetry parameters of these transformations are determined through moving frames that are based on Cartan's method of normalization [44].

In this paper, we extend our earlier works on symmetry preservation in numerical schemes [41,42] and propose a mathematical approach for construction of high-order accurate compact finite-difference schemes that retain Lie symmetry groups of underlying differential equations. One aspect of the proposed method, which is based on equivariant moving frames, is the use of extended symmetry groups of partial differential equations to obtain point transformations not only for independent and dependent variables of differential equations, but also for their derivative terms. Once point transformations for derivatives of differential equations are determined, then these transformations are applied to some (noninvariant) base compact finite-difference schemes (of a desired order of accuracy) to obtain final invariant (or symmetry-preserving) forms of these schemes. Here we note that the unknown symmetry parameters that appear in these point transformations are determined by choosing convenient moving frames for which numerical representations of base schemes simplify notably, and their accuracy improves. The proposed method is applied to some commonly used linear and nonlinear problems, and for all the test problems, the resulting invariant schemes are found to perform significantly better than selected noninvariant base compact schemes in terms of numerical accuracy, verifying the potential advantages of symmetry preservation. We demonstrate the implementation of the proposed method by considering fourth-order accurate invariant compact finite-difference schemes for one-dimensional (1D) and 2D linear advection-diffusion equations, Burgers' equations (i.e., inviscid, viscous, spherical), and shallow water equations. For numerical simplicity, we use forward differencing to discretize temporal derivatives and fourth-order compact schemes based on central differencing to discretize spatial derivatives. Note that the proposed construction of invariant schemes can also be extended to arbitrarily high-order temporal and spatial discretizations. Results obtained from the proposed invariant compact schemes developed for these test problems suggest that symmetry preservation can lead to significant improvements in numerical accuracy, besides storing important geometric information (regarding the underlying differential equations) in associated numerical schemes.

This paper is organized as follows. In Sec. II the formulation for the fourth-order accurate compact schemes along with a detailed discussion on Lie symmetry analysis and invarianti-zation of compact schemes are provided. The step by step development of invariant compact schemes for some linear and nonlinear problems are noted in Sec. III. Performance of the constructed invariant compact schemes along with a detailed discussion of the results obtained from these schemes are presented in Sec. IV. Finally, concluding remarks and a brief summary of the work are given in Sec. V.

II. MATHEMATICAL FORMULATION

In this section, the procedure (that is based on equivariant moving frames) for construction of invariant compact schemes is presented in detail. Brief discussions of Lie symmetry analysis and compact schemes are also included.

A. Construction of compact schemes

Compact finite-difference methods are widely used for high-order computations and in some cases are favored over standard finite-difference methods, due to their ability to achieve high-order accuracy over smaller stencils. For instance, while a standard central difference approximation of the first derivative of a function on a three-point stencil is second-order accurate, an approximation based on a compact scheme (that is also derived through central differencing) of the same derivative could be of higher orders. The implementation of compact schemes is rather simple. To illustrate construction of compact schemes through an example, let us develop fourth-order accurate compact finite-difference schemes for the first and second derivatives of a function U. Consider the following Taylor series expansion of the function U at grid points $(i \pm 1)$:

$$U^{i\pm1} = U^i \pm hU_x^i + \frac{h^2}{2}U_{xx}^i \pm \frac{h^3}{6}U_{xxx}^i + \frac{h^4}{24}U_{(\mathrm{IV})}^i \pm O(h^5),$$

(1)

where h is the discrete spatial step and the symbol $(\cdot)_x$ denotes derivative with respect to variable x. Similarly, the first and second derivatives of U can be expanded in a Taylor series as

$$U_x^{i\pm1} = U_x^i \pm hU_{xx}^i + \frac{h^2}{2}U_{xxx}^i \pm \frac{h^3}{6}U_{(\mathrm{IV})}^i + \frac{h^4}{24}U_{(\mathrm{V})}^i \pm O(h^5),$$

(2)

$$U_{xx}^{i\pm1} = U_{xx}^i \pm hU_{xxx}^i + \frac{h^2}{2}U_{(\mathrm{IV})}^i \pm \frac{h^3}{6}U_{(\mathrm{V})}^i + \frac{h^4}{24}U_{(\mathrm{VI})}^i \pm O(h^5).$$

(3)

In order to eliminate the higher-order derivatives (i.e., $U_{xx}, U_{xxx}, U_{(\mathrm{IV})}$, and $U_{(\mathrm{V})}$) and obtain an implicit relationship between the first derivative U_x and the function U at nodes $i \pm 1$, one can multiply Eq. (1) with constant a at point $i + 1$, and with constant b at point $i - 1$, and multiply Eq. (2) with quantity $c \times h$ at point $i + 1$, and with quantity $d \times h$ at point $i - 1$, and sum up these resulting quantities to obtain the

following equation:

$$aU^{i+1} + bU^{i-1} + chU_x^{i+1} + dhU_x^{i-1} = (a+b)U^i + (a-b+c+d)hU_x^i + (a+b+2c-2d)\frac{h^2}{2}U_{xx}^i + (a-b+3c+3d)\frac{h^3}{6}U_{xxx}^i$$

$$+ (a+b+4c-4d)\frac{h^4}{24}U_{(IV)}^i + (c+d)\frac{h^5}{24}U_{(IV)}^i + O(h^5). \quad (4)$$

The arbitrary constants a, b, c, and d can be obtained via elimination of high-order derivatives as $\{a, b, c, d\} = \{\frac{3}{4}, -\frac{3}{4}, -\frac{1}{4}, -\frac{1}{4}\}$. Hence, the final form of Eq. (4) is

$$\frac{1}{6}U_x^{i+1} + \frac{2}{3}U_x^i + \frac{1}{6}U_x^{i-1} = \frac{U^{i+1} - U^{i-1}}{2h} + O(h^4), \quad (5)$$

which relates the function U to its first derivative and provides a fourth-order accurate implicit approximation for the first derivative of U. Through similar algebraic manipulations, one can obtain the following fourth-order accurate implicit approximation for the second derivative of the function U as well:

$$\frac{1}{12}U_{xx}^{i+1} + \frac{5}{6}U_{xx}^i + \frac{1}{12}U_{xx}^{i-1} = \frac{U^{i+1} - 2U^i + U^{i-1}}{h^2} + O(h^4). \quad (6)$$

Both Eqs. (5) and (6) yield tridiagonal matrices that can easily be solved to accurately approximate the first and second derivatives of U at all grid points. More information on compact schemes along with compact algorithms for derivatives with higher orders of accuracy and a discussion on the treatment of boundary conditions in this approach can be found in the literature [1,2].

B. Lie symmetry analysis

A differential equation is said to possess a symmetry property if one can transform every variable in the equation according to some transformations, such that the resulting output reads exactly the same as the original differential equation in new (transformed) variables. Further, a Lie point symmetry group is an algebraic structure that consists of a set of objects which correspond to continuous symmetries (or coordinate transformations) that map a system to itself with a binary operation that satisfies the following group axioms: (1) closure, (2) existence of identity element, (3) existence of inverse element, and (4) associativity. The procedure for determination of Lie point symmetries of equations is straightforward and well documented in the literature [45–49].

In this context, consider a surface $L(\mathbf{x}, \mathbf{u}, \mathbf{p}) = 0$ to be a partial differential equation, and let the following be a one-parameter (kth-extended) Lie group G:

$$\tilde{x}^j = \tilde{x}^j(\mathbf{x}, \mathbf{u}, s),$$

$$\tilde{u}^i = \tilde{u}^i(\mathbf{x}, \mathbf{u}, s),$$

$$\tilde{u}_{j_1}^i = \tilde{u}_{j_1}^i(\mathbf{x}, \mathbf{u}, \mathbf{u}_1, s), \quad (7)$$

$$\vdots$$

$$\tilde{u}_{j_1 j_2 \ldots j_k}^i = \tilde{u}_{j_1 j_2 \ldots j_k}^i(\mathbf{x}, \mathbf{u}, \mathbf{p}, s),$$

where the arbitrary constant s is the symmetry (or group) parameter, and $\mathbf{p} = (\mathbf{u}_1, \mathbf{u}_2, \ldots, \mathbf{u}_k)$. Here the vectors $\mathbf{x} = (x^1, x^2, \ldots, x^m)$ and $\mathbf{u} = (u^1, u^2, \ldots, u^n)$ denote the independent and dependent variables, respectively, and $\mathbf{u}_k$ represents the vector of all possible kth-order derivatives of $\mathbf{u}$ with respect to the independent variables. Also, the operator $(\cdot)_{j_1 j_2 \cdots j_k}$ represents the partial derivative $\frac{\partial^k (\cdot)}{\partial x_{j_1} \partial x_{j_2} \cdots \partial x_{j_k}}$. The smooth transformation functions $(\tilde{x}^j, \tilde{u}^i, \ldots \tilde{u}_{j_1 j_2 \ldots, j_k}^i)$ given in group G can be further expanded in a Taylor series about the point $s = 0$ to determine the infinitesimal form of the one-parameter Lie group G as

$$\tilde{x}^j = x^j + s[\xi^j(\mathbf{x}, \mathbf{u})] + O(s^2), \quad \xi^j \equiv \left[\frac{\partial \tilde{x}^j}{\partial s}\right]_{s=0},$$

$$\tilde{u}^i = u^i + s[\eta^i(\mathbf{x}, \mathbf{u})] + O(s^2), \quad \eta^i \equiv \left[\frac{\partial \tilde{u}^i}{\partial s}\right]_{s=0},$$

$$\tilde{u}_{j_1}^i = u_{j_1}^i + s\left[\eta_{[j_1]}^i(\mathbf{x}, \mathbf{u}, \mathbf{u}_1)\right] + O(s^2),$$

$$\eta_{[j_1]}^i \equiv \left[\frac{\partial \tilde{u}_{j_1}^i}{\partial s}\right]_{s=0}, \quad (8)$$

$$\vdots$$

$$\tilde{u}_{j_1 j_2 \ldots j_k}^i = u_{j_1 j_2 \ldots j_k}^i + s\left[\eta_{[j_1 \ldots j_k]}^i(\mathbf{x}, \mathbf{u}, \mathbf{p})\right] + O(s^2),$$

$$\eta_{[j_1 \ldots j_k]}^i \equiv \left[\frac{\partial \tilde{u}_{j_1 j_2 \ldots j_k}^i}{\partial s}\right]_{s=0},$$

where ξ^j and η^i are known as the coordinate functions (or the group infinitesimals), which define the transformation of the coordinate variables under the action of the group G. Similarly, $\eta_{[j_1 \ldots j_k]}^i$ is the kth-extended group infinitesimal that defines how the kth derivative is transformed under the action of G and is given by the following relation:

$$\eta_{[j_1 \ldots j_k]}^i = D_{j_k} \eta_{[j_1 \ldots j_{k-1}]}^i - u_{j_1 \ldots j_{k-1} r}^i D_{j_k} \xi^r, \quad (9)$$

where D_{j_k} is the total derivative operator [46].

The surface $L(\mathbf{x}, \mathbf{u}, \mathbf{p}) = 0$ is said to be invariant under the action of the group G if the equation reads the same in new variables:

$$L(\mathbf{x}, \mathbf{u}, \mathbf{p}) = 0 \quad \Leftrightarrow \quad L(\tilde{\mathbf{x}}, \tilde{\mathbf{u}}, \tilde{\mathbf{p}}) = 0. \quad (10)$$

In order to determine the Lie point symmetry group G that will leave the surface $L(\mathbf{x}, \mathbf{u}, \mathbf{p}) = 0$ invariant (or unchanged), the following invariance condition is applied:

$$\mathbf{X}_{[k]} L(\mathbf{x}, \mathbf{u}, \mathbf{p}) = 0, \quad (\text{mod } L = 0), \quad (11)$$

where $\mathbf{X}_{[k]}$ is the k-extended group operator that is of the form

$$\mathbf{X}_{[k]} = \xi^j \frac{\partial}{\partial x^j} + \eta^i \frac{\partial}{\partial u^i} + \cdots + \eta_{[j_1 \ldots j_k]}^i \frac{\partial}{\partial u_{j_1 j_2 \ldots j_k}^i}. \quad (12)$$

Solution of the invariance condition given in Eq. (11) through determination of the coordinate functions yields the Lie point symmetry group G associated with the surface $L(\mathbf{x}, \mathbf{u}, \mathbf{p}) = 0$. A more detailed discussion on Lie symmetry analysis, particularly regarding how to solve the invariance condition, can be found in Ref. [46].

C. Invariantization of compact schemes

In this work, a compact finite-difference scheme [corresponding to a surface $L(\mathbf{z}) = 0$] is considered as an invariant compact scheme if its form remains unchanged under the action of a point symmetry group G associated with the surface $L(\mathbf{z}) = 0$. In this context, let $\tilde{N}_c(\mathbf{z}) = 0$ be an invariant compact finite-difference scheme, and $\tilde{\phi}_c(\mathbf{z}) = 0$ be a stencil equation for the surface $L(\mathbf{z}) = 0$ where $\mathbf{z} = (\mathbf{x}, \mathbf{u}, \mathbf{p})$ is the vector of the independent and dependent variables ($\mathbf{x} = \{x_1, \ldots, x_r\}$, $\mathbf{u} = \{u_1, \ldots, u_s\}$) and derivatives ($\mathbf{p} = \{\partial u_1/\partial x_1, \ldots, \partial u_1/\partial x_r; \ldots; \partial u_s/\partial x_1, \ldots, \partial u_s/\partial x_r\}$), respectively. Here $\mathbf{z}$ is defined on a manifold M that is a subset of the Euclidean space, $M \in R^{r \times s}$. The compact scheme $\tilde{N}_c(\mathbf{z}) = 0$ and the stencil equation $\tilde{\phi}_c(\mathbf{z}) = 0$ are said to be invariant under the action of the group element g (where $g \in G$) if the following condition is satisfied [33,35]:

$$
\begin{aligned}
\tilde{N}_c(\rho(\mathbf{z})\cdot \mathbf{z}) = 0 \quad &\Leftrightarrow \quad \tilde{N}_c(\mathbf{z}) = 0, \\
\tilde{\phi}_c(\rho(\mathbf{z})\cdot \mathbf{z}) = 0 \quad &\Leftrightarrow \quad \tilde{\phi}_c(\mathbf{z}) = 0,
\end{aligned}
\tag{13}
$$

where $\rho(\mathbf{z})$ represents a right moving frame defined on M such that it is a topological map ($\rho : M \to G$) that satisfies the following condition [33]:

$$
\rho(g \cdot \mathbf{z}) = \rho(\mathbf{z}) g^{-1}
$$

for $\forall g \in G$. Here, we note that $\tilde{N} : M^{\diamond n} \to R$, where $M^{\diamond n}$ denotes a joint product manifold which is the off-diagonal part of the Cartesian product $M^{\times n}$ (corresponding to an n-point stencil).

For any given noninvariant compact finite-difference scheme $N_c(\mathbf{z}) = 0$, an invariant form of this scheme $\tilde{N}_c(\mathbf{z}) = 0$ can be obtained by simply transforming every coordinate variable and derivative of the base (noninvariant) compact scheme according to the symmetry group G as $\tilde{N}_c(\mathbf{z}) = N_c(g \cdot \mathbf{z})$ for all $g \in G$. The unknown group parameters (that appear when the action of a particular group element g on the coordinate variables and derivatives is evaluated) can be determined via Cartan's method of normalization. A more detailed discussion on Cartan's method of normalization and equivariant moving frames can be found in the literature [33–35,44].

III. CONSTRUCTION OF INVARIANT NUMERICAL SCHEMES

In this section, the invariantization of compact finite-difference schemes is illustrated through examples. In particular, fourth-order accurate invariant compact schemes are constructed for some linear and nonlinear problems.

A. Inviscid Burgers' equation

As our first test problem, we consider the inviscid Burgers' equation (IBE), which is a model that describes nonlinear wave propagation and is of the form

$$
u_t + u\, u_x = 0.
\tag{14}
$$

A noninvariant compact scheme can be constructed for the IBE using the compact algorithms developed for the spatial first, Eq. (5), and second, Eq. (6), derivatives. As for the time derivative, for simplicity, a classical first-order forward differencing technique can be considered. The order of accuracy can be improved from first to second order via truncation error analysis or defect correction. Hence the final form of the compact scheme for the inviscid Burgers' equation, at (x^i, t^n), can be expressed as

$$
N_c(\mathbf{z}) = \frac{u^{(i,n+1)} - u^{(i,n)}}{\tau} + u^{(i,n)}u_x^{(i,n)} + d_c = 0.
\tag{15}
$$

Here d_c represents the defect correction terms (obtained from truncation error analysis) that are added to the scheme to improve accuracy and is given by

$$
d_c = -\frac{\tau}{2}\left[\left(u^{(i,n)}\right)^2 u_{xx}^{(i,n)} + 2\, u^{(i,n)}\left(u_x^{(i,n)}\right)^2\right] + O(\tau^2, h^4),
\tag{16}
$$

where τ and h denote the discrete time and space steps, respectively. Also, the terms $u_x^{(i,n)}$ and $u_{xx}^{(i,n)}$ denote the numerical representations for the first and second derivatives, at (x^i, t^n), based on the compact schemes given in Eqs. (5) and (6).

Further, the symmetry group G associated with the inviscid Burgers' equation can be found (via Lie symmetry analysis) as

$$
\begin{aligned}
X_1 &= t^2 \frac{\partial}{\partial t} + x\, t \frac{\partial}{\partial x} + (x - t\, u) \frac{\partial}{\partial u}, \\
X_2 &= t\, x \frac{\partial}{\partial t} + x^2 \frac{\partial}{\partial x} + u\,(x - t\, u) \frac{\partial}{\partial u}, \\
X_3 &= 2t \frac{\partial}{\partial t} + x \frac{\partial}{\partial x} - u \frac{\partial}{\partial u}, \\
X_4 &= x \frac{\partial}{\partial t} - u^2 \frac{\partial}{\partial u}, \\
X_5 &= t \frac{\partial}{\partial x} + \frac{\partial}{\partial u}, \\
X_6 &= \frac{\partial}{\partial t}, \\
X_7 &= \frac{\partial}{\partial x},
\end{aligned}
\tag{17}
$$

where $X_{r=1,\ldots,7}$, is the group operator that corresponds to that particular subgroup. The point transformations, $\tilde{\mathbf{z}} = (\tilde{t}, \tilde{x}, \tilde{u}, \tilde{\mathbf{p}})$, associated with a particular subgroup can be found using Lie series expansion as follows:

$$
\tilde{z}_i = e^{(s_j X_j)} z_i = z_i + s_j\,(X_j z_i) + \frac{s_j^2}{2!} X_j(X_j z_i)
$$
$$
+ \frac{s_j^3}{3!} X_j[X_j(X_j z_i)] + \cdots.
\tag{18}
$$

Here we note that in order to find the extended point transformations $\tilde{\mathbf{p}} = (\tilde{u}_{\tilde{x}}, \tilde{u}_{\tilde{x}\tilde{x}})$, one should extend the group operators given in Eq. (17) such that it accounts for all the derivative terms before these groups are used in the Lie series given in Eq. (18). Alternatively, one can use the chain rule to find the extended point transformations. For instance, the

transformation expression for the spatial first derivative can be found using

$$\frac{\partial \tilde{u}}{\partial \tilde{x}} = \frac{\partial \tilde{u}}{\partial x}\frac{\partial x}{\partial \tilde{x}} + \frac{\partial \tilde{u}}{\partial t}\frac{\partial t}{\partial \tilde{x}}$$

once the point transformations for the independent and dependent variables are found. Similarly, point transformations associated with a multiple number of subgroups can be obtained by substituting each subgroup into Eq. (18) in an arbitrary order. Although it is desirable to obtain point transformations based on all the Lie groups associated with a partial differential equation (PDE), such an approach could lead to cumbersome numerical representations [42]. In view of this difficulty, it is sometimes reasonable to only consider selected subgroups without significant loss of accuracy. Hence, in the context of the current example problem, we only choose the subgroups X_1, X_3, X_6, and X_7 for preservation in the associated (noninvariant) compact scheme given in Eq. (15). The global transformations obtained from these particular subgroups are found via Eq. (18) as

$$\tilde{t} = e^{2s_3}\frac{(t + s_6)}{\lambda},$$

$$\tilde{x} = e^{s_3}\frac{x + s_7}{\lambda},$$

$$\tilde{u} = e^{-s_3}[\lambda u + s_1(x + s_7)], \qquad (19)$$

$$\tilde{u}_{\tilde{x}} = e^{-2s_3}(\lambda^2 u_x + s_1\lambda),$$

$$\tilde{u}_{\tilde{x}\tilde{x}} = e^{-3s_3}\lambda^3 u_{xx},$$

where $\lambda = 1 - s_1(t + s_6)$. The compact scheme constructed for the inviscid Burgers' equation, Eq. (15), can be invariantized by transforming every coordinate variable and derivative according to the above transformations:

$$\tilde{N}_c(\mathbf{z}) = N_c(g \cdot \mathbf{z}) = \frac{\tilde{u}^{(i,n+1)} - \tilde{u}^{(i,n)}}{\tilde{\tau}} + \tilde{u}^{(i,n)}\tilde{u}_{\tilde{x}}^{(i,n)}$$
$$- \frac{\tilde{\tau}}{2}\Big[(\tilde{u}^{(i,n)})^2\,\tilde{u}_{\tilde{x}\tilde{x}}^{(i,n)} + 2\,\tilde{u}^{(i,n)}\big(\tilde{u}_{\tilde{x}}^{(i,n)}\big)^2\Big] = 0. \qquad (20)$$

Based on the point transformations given in Eq. (19), it appears that the symmetry parameter s_3 does not appear in the transformed scheme given in Eq. (20). All the other symmetry parameters can be determined through Cartan's method of normalization. First, we consider convenient normalization conditions that lead to simple stencils. For instance, normalization conditions $\tilde{t}^{(i,n)} = 0$ and $\tilde{x}^{(i,n)} = 0$, among infinite possibilities, yield a simple stencil where the symmetry parameters s_6 and s_7 are $-t^{(i,n)}$ and $-x^{(i,n)}$, respectively. Second, we choose normalization conditions that remove terms from the truncation error of compact schemes under consideration and hence lead to a considerable improvement in numerical accuracy, besides simplifying their numerical representations [42]. In this context, the normalization condition $\tilde{u}_{\tilde{x}}^{(i,n)} = 0$ can be used to determine the symmetry parameter s_1,

$$\tilde{u}_{\tilde{x}}^{(i,n)} = 0 \quad \Rightarrow \quad u_x^{(i,n)} + s_1 = 0 \quad \Rightarrow \quad s_1 = -u_x^{(i,n)}, \qquad (21)$$

as this particular normalization condition removes all the terms that include the spatial first derivative from the compact

scheme given in Eq. (20) in the transformed space as shown in the following:

$$\tilde{N}_c(\mathbf{z}) = N_c(g \cdot \mathbf{z}) = \frac{\tilde{u}^{(i,n+1)} - \tilde{u}^{(i,n)}}{\tilde{\tau}}$$
$$- \frac{\tilde{\tau}}{2}(\tilde{u}^{(i,n)})^2\,\tilde{u}_{\tilde{x}\tilde{x}}^{(i,n)} + O(\tilde{\tau}^2, \tilde{h}^4) = 0. \qquad (22)$$

The compact scheme given in Eq. (22) is invariant under the symmetry groups X_1, X_3, X_6, and X_7 and can also be expressed in original variables:

$$u^{(i,n+1)} = \frac{1}{\lambda_{n+1}}\Bigg[u^{(i,n)} + \frac{\tau^2}{2\lambda_{n+1}^2}\big(u^{(i,n)}\big)^2 u_{xx}^{(i,n)}\Bigg], \qquad (23)$$

where $\lambda_{n+1} = 1 - s_1\tau$ and $u_{xx}^{(i,n)}$ represents the fourth-order compact approximation of the second derivative given in Eq. (6). Note that for most of the test problems considered in this work, we use a time-space orthogonal mesh, $t^{(i+1,n)} - t^{(i,n)} = 0$ and $x^{(i,n+1)} - x^{(i,n)} = 0$, and hence, for simplicity, we will replace $t^{(i,n)}$ with t^n, and $x^{(i,n)}$ with x^i in the following examples. Invariance of the compact scheme constructed for the inviscid Burgers' equation, Eq. (23), can be verified by transforming every variable in this scheme according to the transformations given in Eq. (19),

$$\tilde{u}^{(i,n+1)} = \frac{1}{\tilde{\lambda}_{n+1}}\Bigg[\tilde{u}^{(i,n)} + \frac{\tilde{\tau}^2}{2\tilde{\lambda}_{n+1}^2}\big(\tilde{u}^{(i,n)}\big)^2\tilde{u}_{\tilde{x}\tilde{x}}^{(i,n)}\Bigg],$$

and the resulting transformed scheme should be identical to Eq. (23) as demonstrated below:

$$\tilde{\lambda}_{n+1} = 1 - \tilde{u}_{\tilde{x}}\tilde{\tau} = 1,$$

$$\tilde{\tau} = e^{2s_3}\frac{\tau}{\lambda_{n+1}},$$

$$\tilde{u}^{(i,n+1)} = e^{-s_3}\big[\lambda_{n+1}u^{(i,n+1)} + s_1\big(x^{(i,n+1)} - x^{(i,n)}\big)\big]$$
$$= e^{-s_3}\lambda_{n+1}u^{(i,n+1)},$$

$$\tilde{u}^{(i,n)} = e^{-s_3}\big[u^{(i,n)} + s_1\big(x^{(i,n)} - x^{(i,n)}\big)\big] = e^{-s_3}u^{(i,n)},$$

$$\tilde{u}_{\tilde{x}\tilde{x}}^{(i,n)} = e^{-3s_3}u_{xx}^{(i,n)}.$$

Substitution of the above relations into the transformed form of Eq. (23) does in fact result in Eq. (23) and hence verifies the invariance of Eq. (23) under the selected symmetry groups.

Here we also note that for this particular problem, for simplicity, we considered first-order forward differencing for the time derivative and used the method of modified equations to improve the accuracy of the approximation from first to second order. However, one could also use higher-order approximations or other discretization techniques (i.e., Runge-Kutta methods) for the time derivative if desired. A particularly interesting case occurs when a TVD-RK2 discretization scheme (from Ref. [50]) is used for the time derivative in Eq. (15). In this case, the final form of the invariant compact scheme constructed using the transformations and moving

frames considered for the IBE would be identical to the invariant compact scheme given in Eq. (23).

B. Linear advection-diffusion equation in one dimension

As our second test problem, we choose the 1D linear advection-diffusion equation of the form

$$u_t + \alpha u_x = \nu u_{xx}, \tag{24}$$

which describes the evolution of a quantity u due to linear advection and diffusion processes. The symbols α and ν denote the constant characteristic speed and diffusion coefficient, respectively. A noninvariant compact numerical scheme can be developed for Eq. (24) as

$$\frac{u^{(i,n+1)} - u^{(i,n)}}{\tau} + \alpha u_x^{(i,n)} = \nu u_{xx}^{(i,n)}, \tag{25}$$

where forward differencing is considered for the time derivative, and the spatial first and second derivatives are approximated according to Eqs. (5) and (6), respectively. The symmetry group G associated with the 1D advection-diffusion equation is

$$X_1 = 2 t^2 \frac{\partial}{\partial t} + 2 x t \frac{\partial}{\partial x} - u \left(t + \frac{(x - \alpha t)^2}{2 \nu} \right) \frac{\partial}{\partial u},$$

$$X_2 = 4 t \frac{\partial}{\partial t} + 2 (x + \alpha t) \frac{\partial}{\partial x},$$

$$X_3 = t \frac{\partial}{\partial x} - u \frac{(x - \alpha t)}{2 \nu} \frac{\partial}{\partial u},$$

$$X_4 = u \frac{\partial}{\partial u}, \tag{26}$$

$$X_5 = \frac{\partial}{\partial t},$$

$$X_6 = \frac{\partial}{\partial x},$$

$$X_\infty = \alpha(t, x) \frac{\partial}{\partial u},$$

where X_∞ represents an infinite dimensional symmetry group and $\alpha(t, x)$ is a solution of Eq. (24). Considering the subgroups X_1, X_5, and X_6, the following point transformations can be obtained:

$$\tilde{t} = \frac{t + s_5}{\lambda}, \quad \tilde{x} = \frac{x + s_6}{\lambda},$$

$$\tilde{u} = \lambda^{\frac{1}{2}} u \, \exp\left(-\frac{s_1 \gamma^2}{2\lambda\nu}\right),$$

$$\tilde{u}_{\tilde{x}} = \lambda^{\frac{1}{2}} \nu^{-1}(s_1\gamma u + \lambda\nu u_x) \, \exp\left(-\frac{s_1 \gamma^2}{2\lambda\nu}\right), \tag{27}$$

$$\tilde{u}_{\tilde{x}\tilde{x}} = \lambda^{\frac{1}{2}} \nu^{-2}\big(s_1^2\gamma^2 u - s_1\lambda\nu u - 2s_1\lambda\gamma\nu u_x + \lambda^2\nu^2 u_{xx}\big)$$

$$\times \, \exp\left(-\frac{s_1 \gamma^2}{2\lambda\nu}\right),$$

where $\lambda = 1 - 2 s_1 (t + s_5)$ and $\gamma = x + s_6 - \alpha (t + s_5)$. The other subgroups are neglected as their inclusion leads to point transformations of cumbersome structures that are difficult to implement. The normalization conditions $\tilde{t}^n = 0$ and $\tilde{x}^i = 0$ can be used to determine the symmetry parameters s_5 and

s_6, respectively. The symmetry parameter s_1 (corresponding to the projection group X_1) can be found by considering the normalization condition:

$$\tilde{u}_{\tilde{x}\tilde{x}}^{(i,n)} = 0 \quad \Rightarrow \quad s_1 = \frac{\nu}{u^{(i,n)}} u_{xx}^{(i,n)}. \tag{28}$$

As all the unknown symmetry parameters are defined, the point transformations given in Eq. (27) can be implemented to the base compact numerical scheme, Eq. (25). This implementation reduces the scheme to a form of linear advection equation in the transformed space:

$$\frac{\tilde{u}^{(i,n+1)} - \tilde{u}^{(i,n)}}{\tilde{\tau}} + \alpha \, \tilde{u}_{\tilde{x}}^{(i,n)} = 0, \tag{29}$$

where the spatial second derivative is removed from the scheme owing to the normalization condition given in Eq. (28). Hence, the transformed compact scheme given in Eq. (29) that is constructed for the 1D linear advection-diffusion equation and is invariant under the subgroups X_1, X_5, and X_6 can be expressed in the original discrete variables as

$$u^{(i,n+1)} = \lambda_{n+1}^{-\frac{3}{2}} \left(\lambda_{n+1} u^{(i,n)} - \tau \, \alpha \, u_x^{(i,n)} \right) \exp\left(\frac{s_1 \alpha^2 \tau^2}{2\nu \lambda_{n+1}} \right), \tag{30}$$

where $\lambda_{n+1} = 1 - 2s_1\tau$. Note that in Eq. (30), the derivative $u_x^{(i,n)}$ is obtained using the compact representation given in Eq. (5) and associated matrix solutions.

While stability analysis of traditional (noninvariant) linear compact schemes is a straightforward procedure [2], similar stability analysis of invariant compact schemes [as in Eq. (30)] is not so straightforward. The difficulty in stability analysis with invariant schemes is due to the choice of the local moving frames and the associated parameters and variables (i.e., s_1), which could bring in additional nonlinearities. Although we observed qualitatively similar behavior for both noninvariant compact schemes and their invariant counterparts, more rigorous analysis (outside the scope of this paper) is needed for accurately quantifying stability criteria of our proposed invariant schemes. Further, for invariant compact schemes, it can be shown that the results of modified wavenumber analysis are identical to that of corresponding base noninvariant compact schemes.

C. Viscous Burgers' equation in one dimension

As our third test problem, let us consider the viscous Burgers' equation that is of the form

$$u_t + u u_x = \nu u_{xx} \tag{31}$$

and develop an invariant compact numerical scheme for this particular PDE. Similar to the 1D linear advection-diffusion equation, we consider forward differencing for the time derivative and use Eqs. (5) and (6) for the spatial derivatives to construct the noninvariant base compact scheme for the solution of this PDE as

$$\frac{u^{(i,n+1)} - u^{(i,n)}}{\tau} + u^{(i,n)} u_x^{(i,n)} = \nu u_{xx}^{(i,n)}. \tag{32}$$

The symmetry group G associated with the viscous Burgers' equation is

$$
X_1 = t^2 \frac{\partial}{\partial t} + x t \frac{\partial}{\partial x} + (x - t u) \frac{\partial}{\partial u},
$$

$$
X_2 = t \frac{\partial}{\partial x} + \frac{\partial}{\partial u}
$$

$$
X_3 = 2t \frac{\partial}{\partial t} + x \frac{\partial}{\partial x} - u \frac{\partial}{\partial u}, \tag{33}
$$

$$
X_4 = \frac{\partial}{\partial t},
$$

$$
X_5 = \frac{\partial}{\partial x}.
$$

The point transformations that account for the projection group X_1, Galilean transformation group X_2, scaling group X_3, and translation groups X_4 and X_5 can be found as

$$
\tilde{t} = e^{2s_3} \frac{(t + s_4)}{\lambda},
$$

$$
\tilde{x} = e^{s_3} \frac{x + s_5 + s_2(t + s_4)}{\lambda},
$$

$$
\tilde{u} = e^{-s_3}(\lambda u + s_1(x + s_5) + s_2), \tag{34}
$$

$$
\tilde{u}_{\tilde{x}} = e^{-2s_3}(\lambda^2 u_x + s_1 \lambda),
$$

$$
\tilde{u}_{\tilde{x}\tilde{x}} = e^{-3s_3} \lambda^3 u_{xx},
$$

where $\lambda = 1 - s_1(t + s_4)$. As similar to the inviscid Burgers' equation, the scaling symmetry parameter s_3 does not occur when these transformations are implemented to the compact scheme given in Eq. (32). The symmetry parameters associated with the translation groups X_4 and X_5 can be found by considering the same normalization conditions used for the previous problems. The Galilean parameter s_2 can be found by using the normalization condition $\tilde{u}^{(i,n)} = 0$. And, finally, the projection parameter s_1 can be found by choosing a moving frame for which the approximation for the first derivative goes to zero in the transformed space:

$$
\tilde{u}_{\tilde{x}}^{(i,n)} = 0 \quad \Rightarrow \quad s_1 = -u_x^{(i,n)}. \tag{35}
$$

The above normalization condition indicates that all terms in the base (noninvariant) compact scheme, Eq. (32), that include the spatial first derivative will be removed from the compact scheme in the transformed space leading to the following reduced form:

$$
\tilde{u}^{(i,n+1)} = \nu \, \tilde{\tau} \, \tilde{u}_{\tilde{x}\tilde{x}}^{(i,n)}, \tag{36}
$$

where $\tilde{\tau} = \tilde{t}^{(i,n+1)}$. The transformed compact numerical scheme, Eq. (36), that is invariant under all the symmetry groups of the viscous Burgers' equation can also be expressed in original variables as

$$
u^{(i,n+1)} = \frac{1}{\lambda_{n+1}} \left[u^{(i,n)} - s_1\left(x^{(i,n+1)} - x^{(i,n)}\right) + \frac{\tau \nu}{\lambda_{n+1}} u_{xx}^{(i,n)} \right], \tag{37}
$$

where $\lambda_{n+1} = 1 - s_1 \tau$.

D. Advection-diffusion equation in two dimensions

As our fourth test problem, we choose the 2D linear advection-diffusion equation that is of the form

$$
u_t + \alpha u_x + \beta u_y = \nu(u_{xx} + u_{yy}) \tag{38}
$$

to demonstrate the applicability of the proposed method to a multidimensional problem. Here α and β denote constant characteristic wave speeds along x and y coordinates, respectively. For this particular PDE, two different compact numerical schemes that are invariant under the same symmetry groups, but are constructed using different moving frames, are developed. Similar to the previous problems, the base (noninvariant) compact numerical scheme considered for this PDE is also developed considering forward differencing for the temporal derivative and fourth-order compact finite-difference algorithms, given in Eqs. (5) and (6), for the spatial derivatives:

$$
\frac{u^{(i,j,n+1)} - u^{(i,j,n)}}{\tau} + \alpha u_x^{(i,j,n)} + \beta u_y^{(i,j,n)}
$$
$$
= \nu\left(u_{xx}^{(i,j,n)} + u_{yy}^{(i,j,n)}\right). \tag{39}
$$

Considering the symmetry group associated with the 2D linear advection-diffusion equation,

$$
X_1 = 4 \nu t^2 \frac{\partial}{\partial t} + 4 \nu x t \frac{\partial}{\partial x} + 4 \nu y t \frac{\partial}{\partial y}
$$
$$
- u [(x - \alpha t)^2 + (y - \beta t)^2 + 4\nu t] \frac{\partial}{\partial u},
$$

$$
X_2 = 2 \nu t \frac{\partial}{\partial x} + 2 \nu t \frac{\partial}{\partial y} - u (x - \alpha t + y - \beta t) \frac{\partial}{\partial u},
$$

$$
X_3 = 2 \nu y \frac{\partial}{\partial x} - 2 \nu x \frac{\partial}{\partial y} - u (\beta x - \alpha y) \frac{\partial}{\partial u},
$$

$$
X_4 = 4 \nu t \frac{\partial}{\partial t} + 2\nu x \frac{\partial}{\partial x} + 2\nu y \frac{\partial}{\partial y}
$$
$$
+ u[\alpha(x - \alpha t) + \beta(y - \beta t)] \frac{\partial}{\partial u},
$$

$$
X_5 = u \frac{\partial}{\partial u},
$$

$$
X_6 = \frac{\partial}{\partial t},
$$

$$
X_7 = \frac{\partial}{\partial x},
$$

$$
X_8 = \frac{\partial}{\partial y}, \tag{40}
$$

the following point transformations that are based on the subgroups X_1, X_6, X_7, and X_8, are found:

$$
\tilde{t} = \frac{t + s_6}{\lambda}, \quad \tilde{x} = \frac{x + s_7}{\lambda}, \quad \tilde{y} = \frac{y + s_8}{\lambda},
$$

$$
\tilde{u} = \lambda u \exp\left[-\frac{s_1(\gamma^2 + \theta^2)}{\lambda}\right]
$$

$$
\tilde{u}_{\tilde{x}} = (2 \lambda \gamma s_1 u + \lambda^2 u_x) \exp\left[-\frac{s_1(\gamma^2 + \theta^2)}{\lambda}\right],
$$

$$
\tilde{u}_{\tilde{y}} = (2 \lambda \theta s_1 u + \lambda^2 u_y) \exp\left[-\frac{s_1(\gamma^2 + \theta^2)}{\lambda}\right],
$$

$$\tilde{u}_{\tilde{x}\tilde{x}} = \left(4\lambda\gamma^2 s_1^2 u - 2\lambda^2 s_1 u + 4\lambda^2\gamma s_1 u_x + \lambda^3 u_{xx}\right)$$

$$\times \exp\left[-\frac{s_1(\gamma^2+\theta^2)}{\lambda}\right],$$

$$\tilde{u}_{\tilde{y}\tilde{y}} = \left(4\lambda\theta^2 s_1^2 u - 2\lambda^2 s_1 u + 4\lambda^2\theta s_1 u_y + \lambda^3 u_{yy}\right)$$

$$\times \exp\left[-\frac{s_1(\gamma^2+\theta^2)}{\lambda}\right], \tag{41}$$

where

$$\lambda = 1 - 4\nu s_1(t+s_6),$$
$$\gamma = x + s_7 - \alpha(t+s_6),$$
$$\theta = y + s_8 - \beta(t+s_6).$$

The base compact scheme given in Eq. (39) can be transformed according to the above transformations as follows:

$$\frac{\tilde{u}^{(i,j,n+1)} - \tilde{u}^{(i,j,n)}}{\tilde{\tau}} + \alpha\tilde{u}_{\tilde{x}}^{(i,j,n)} + \beta\tilde{u}_{\tilde{y}}^{(i,j,n)}$$

$$= \nu\left(\tilde{u}_{\tilde{x}\tilde{x}}^{(i,j,n)} + \tilde{u}_{\tilde{y}\tilde{y}}^{(i,j,n)}\right). \tag{42}$$

Here we note that, for simplicity, we ignore the Galilean (X_2 and X_3) and scaling (X_4 and X_5) groups and do not consider them for determination of the point transformations as their inclusion (besides the other symmetry groups) result in transformations that are laborious to implement. The symmetry parameters s_6, s_7, and s_8 can be determined by considering the normalization conditions $\tilde{t}^n = 0$, $\tilde{x}_i = 0$, and $\tilde{y}_j = 0$, respectively. As for the determination of the symmetry parameter s_1, we consider two different normalization conditions to evaluate the effect of these selections on the numerical accuracy of the resulting invariant schemes. We choose

$$\tilde{u}_{\tilde{x}\tilde{x}}^{(i,j,n)} = 0 \quad \Rightarrow \quad s_1 = \frac{u_{xx}^{(i,j,n)}}{2u^{(i,j,n)}} \tag{43}$$

as the first normalization condition and construct an invariant compact scheme (referred to as SYM-1) as

$$\frac{\tilde{u}^{(i,j,n+1)} - \tilde{u}^{(i,j,n)}}{\tilde{\tau}} + \alpha\tilde{u}_{\tilde{x}}^{(i,j,n)} + \beta\tilde{u}_{\tilde{y}}^{(i,j,n)} = \nu\tilde{u}_{\tilde{y}\tilde{y}}^{(i,j,n)}. \tag{44}$$

In the second case, we consider the normalization condition

$$\tilde{u}_{\tilde{x}\tilde{x}}^{(i,j,n)} + \tilde{u}_{\tilde{y}\tilde{y}}^{(i,j,n)} = 0 \quad \Rightarrow \quad s_1 = \frac{u_{xx}^{(i,j,n)} + u_{yy}^{(i,j,n)}}{4u^{(i,j,n)}} \tag{45}$$

and construct another invariant compact scheme (referred to as SYM-2) as

$$\frac{\tilde{u}^{(i,j,n+1)} - \tilde{u}^{(i,j,n)}}{\tilde{\tau}} + \alpha\tilde{u}_{\tilde{x}}^{(i,j,n)} + \beta\tilde{u}_{\tilde{y}}^{(i,j,n)} = 0. \tag{46}$$

Here we note that both Eqs. (44) and (46) can also be expressed in the original variables by implementing the transformations given in Eq. (41).

E. Viscous Burgers' equation in two dimensions

As our fifth test problem, we consider the 2D viscous Burgers' equation of the form

$$u_t + u\,u_x + v\,u_y = \nu(u_{xx} + u_{yy}), \tag{47}$$

$$v_t + u\,v_x + v\,v_y = \nu(v_{xx} + v_{yy}), \tag{48}$$

where u and v represent velocity components in x and y coordinates, respectively. A noninvariant base compact scheme selected for this problem has the following form:

$$\frac{u^{(i,j,n+1)} - u^{(i,j,n)}}{\tau} + u^{(i,j,n)}u_x^{(i,j,n)} + v^{(i,j,n)}u_y^{(i,j,n)}$$

$$= \nu\left(u_{xx}^{(i,j,n)} + u_{yy}^{(i,j,n)}\right), \tag{49}$$

$$\frac{v^{(i,j,n+1)} - v^{(i,j,n)}}{\tau} + u^{(i,j,n)}v_x^{(i,j,n)} + v^{(i,j,n)}v_y^{(i,j,n)}$$

$$= \nu\left(v_{xx}^{(i,j,n)} + v_{yy}^{(i,j,n)}\right), \tag{50}$$

where the temporal derivative is approximated via forward differencing, and the spatial derivatives are approximated via the fourth-order compact algorithms given in Eqs. (5) and (6).

Similar to the previous problems, the first step in the invariantization procedure is to determine the symmetries of the PDE under consideration. In this case, the 2D viscous Burgers' equation admits the following eight-parameter Lie group:

$$X_1 = t^2\frac{\partial}{\partial t} + xt\frac{\partial}{\partial x} + yt\frac{\partial}{\partial y}$$

$$\quad + (x - tu)\frac{\partial}{\partial u} + (y - tv)\frac{\partial}{\partial v},$$

$$X_2 = 2t\frac{\partial}{\partial t} + x\frac{\partial}{\partial x} + y\frac{\partial}{\partial y} - u\frac{\partial}{\partial u} - v\frac{\partial}{\partial v},$$

$$X_3 = y\frac{\partial}{\partial x} - x\frac{\partial}{\partial y} + v\frac{\partial}{\partial u} - u\frac{\partial}{\partial v},$$

$$X_4 = t\frac{\partial}{\partial x} + \frac{\partial}{\partial u}, \tag{51}$$

$$X_5 = t\frac{\partial}{\partial y} + \frac{\partial}{\partial v},$$

$$X_6 = \frac{\partial}{\partial x},$$

$$X_7 = \frac{\partial}{\partial y},$$

$$X_8 = \frac{\partial}{\partial t}.$$

The extended point transformation group associated with group operators X_1, X_2, X_4, X_5, X_6, X_7, and X_8 is as follows:

$$\tilde{t} = e^{2s_2}\frac{(t+s_8)}{1 - s_1(t+s_8)},$$

$$\tilde{x} = e^{s_2}\frac{x + s_6 + s_4(t+s_8)}{1 - s_1(t+s_8)},$$

$$\tilde{y} = e^{s_2}\frac{y + s_7 + s_5(t+s_8)}{1 - s_1(t+s_8)},$$

$$\tilde{u} = e^{-s_2}\{[1 - s_1(t+s_8)]u + s_1(x+s_6) + s_4\},$$

$$\tilde{v} = e^{-s_2}\{[1 - s_1(t+s_8)]v + s_1(y+s_7) + s_5\},$$

$$\tilde{u}_{\tilde{x}} = e^{-2s_2}\{[1 - s_1(t+s_8)]^2 u_x + s_1[1 - s_1(t+s_8)]\},$$

$$\tilde{u}_{\tilde{y}} = e^{-2s_2}\{[1 - s_1(t+s_8)]^2 u_y\},$$

$$\tilde{u}_{\tilde{x}\tilde{x}} = e^{-3s_2}\{[1 - s_1(t+s_8)]^3 u_{xx}\},$$

$$\tilde{u}_{\tilde{y}\tilde{y}} = e^{-3s_2}\{[1 - s_1\,(t + s_8)]^3 u_{yy}\},$$

$$\tilde{v}_{\tilde{x}} = e^{-2s_2}\{[1 - s_1\,(t + s_8)]^2 v_x\},$$

$$\tilde{v}_{\tilde{y}} = e^{-2s_2}\{[1 - s_1\,(t + s_8)]^2 v_y + s_1[1 - s_1\,(t + s_8)]\},$$

$$\tilde{v}_{\tilde{x}\tilde{x}} = e^{-3s_2}\{[1 - s_1\,(t + s_8)]^3 v_{xx}\},$$

$$\tilde{v}_{\tilde{y}\tilde{y}} = e^{-3s_2}\{[1 - s_1\,(t + s_8)]^3 v_{yy}\}, \tag{52}$$

where the rotation group X_3 is ignored for the sake of simplicity. The next step is to determine the unknown symmetry parameters (i.e., s_1, s_3, s_4, s_5, s_6, s_7, and s_8) via Cartan's method of normalization. Similar to the previous problems, to determine the symmetry parameters s_6, s_7 and s_8, we use the normalization conditions that lead to simple stencils (i.e., $\tilde{x}_i^n = 0$, $\tilde{y}_j^n = 0$ and $\tilde{t}^n = 0$). The scaling symmetry parameter s_2 does not appear in the transformed base compact scheme. The Galilean parameters s_4 and s_5 are ignored for this problem for the sake of simplicity. Note that we previously demonstrated the preservation of such groups in the case of the 1D viscous Burgers' equation in Sec. III C. However, if one desires to preserve these symmetry groups as well, they can simply consider convenient normalization conditions to determine the relevant symmetry parameters and take it from there. Here we note that inclusion of these symmetry groups will lead to a cumbersome numerical representation and will require use of a nonorthogonal stencil as was the case for the 1D viscous Burgers' equation. As for the projection symmetry parameter s_1, we can choose two different (convenient) normalization conditions: (1) one that removes the nonlinear transport terms in Eq. (49) and (2) one that removes the nonlinear transport terms in Eq. (50):

$$\tilde{u}^{(i,j,n)}\,\tilde{u}_{\tilde{x}}^{(i,j,n)} + \tilde{v}^{(i,j,n)}\,\tilde{u}_{\tilde{y}}^{(i,j,n)} = 0$$

$$\Leftrightarrow \quad \widehat{s}_1 = -u_x^{(i,j,n)} - \frac{v^{(i,j,n)}}{u^{(i,j,n)}}u_y^{(i,j,n)}, \tag{53}$$

$$\tilde{u}^{(i,j,n)}\,\tilde{v}_{\tilde{x}}^{(i,j,n)} + \tilde{v}^{(i,j,n)}\,\tilde{v}_{\tilde{y}}^{(i,j,n)} = 0$$

$$\Leftrightarrow \quad \overline{s}_1 = -v_y^{(i,j,n)} - \frac{u^{(i,j,n)}}{v^{(i,j,n)}}v_x^{(i,j,n)}. \tag{54}$$

Based on these symmetry parameters, the final form of the fourth-order accurate invariant compact scheme that is constructed for the 2D viscous Burgers' equation is found as follows:

$$\frac{\widehat{u}^{(i,j,n+1)} - \widehat{u}^{(i,j,n)}}{\widehat{\tau}} = \nu\big(\widehat{u}_{\tilde{x}\tilde{x}}^{(i,j,n)} + \widehat{u}_{\tilde{y}\tilde{y}}^{(i,j,n)}\big), \tag{55}$$

$$\frac{\overline{v}^{(i,j,n+1)} - \overline{v}^{(i,j,n)}}{\overline{\tau}} = \nu\big(\overline{v}_{\tilde{x}\tilde{x}}^{(i,j,n)} + \overline{v}_{\tilde{y}\tilde{y}}^{(i,j,n)}\big), \tag{56}$$

where the symbols $\widehat{(\cdot)}$ and $\overline{(\cdot)}$ represent different transformations corresponding to s_1 definitions given in Eqs. (53) and (54), respectively.

F. Spherical Burgers' equation in one dimension

To further evaluate the performance of the proposed invariant schemes in the case of nonlinear problems, we demonstrate the implementation of the method to the spherical

Burgers' equation that is of the form

$$u_t + \frac{u}{t} + uu_x + u_{xx} = 0 \tag{57}$$

and develop a fourth-order accurate invariant compact scheme for this problem as well. The symmetry properties of this PDE along with a constructed invariant finite-difference scheme (developed for this PDE) are also presented in Ref. [51]. In this work, we approach this problem from a compact finite differencing point of view and construct a fourth-order accurate invariant compact scheme for this PDE. The point transformations obtained from the full Lie symmetry group associated with this PDE can be found as

$$\tilde{x} = e^{s_1}(x + s_2 \ln t) + s_3,$$

$$\tilde{t} = e^{2s_1}t,$$

$$\tilde{u} = e^{-s_1}\left(u + \frac{s_2}{t}\right), \tag{58}$$

$$\tilde{u}_{\tilde{x}} = e^{-2s_1}u_x,$$

$$\tilde{u}_{\tilde{x}\tilde{x}} = e^{-3s_1}u_{xx}.$$

Considering the same normalization conditions described in Ref. [51],

$$\tilde{x}^{(i,n)} = 0,$$

$$\tilde{t}^{(i,n)} = 1,$$

$$\tilde{u}^{(i,n)} = 0,$$

$$\tilde{x}^{(i,n+1)} - \tilde{x}^{(i,n)} = 0, \tag{59}$$

we can obtain the final form of the fourth-order accurate invariant compact scheme for this PDE as

$$u^{(i,n+1)} = u^{(i,n)}\frac{t^n}{t^{n+1}} - \tau u_{xx}^{(i,n)}, \tag{60}$$

where the solution stencil is nonorthogonal and given by the following relation:

$$x^{(i,n+1)} - x^{(i,n)} = t^n u^{(i,n)} \ln\left(\frac{t^{n+1}}{t^n}\right).$$

Performance of the invariant scheme, given in Eq. (60), that preserves the full Lie symmetry group associated with the 1D spherical Burger's equation is evaluated in Sec. IV.

G. Shallow water equations in two dimensions

As our next test case, to show the implementation of the proposed method to multidimensional nonlinear problems, we consider the 2D shallow water equations given as

$$u_t + uu_x + vu_y + gh_x = 0, \tag{61}$$

$$v_t + uv_x + vv_y + gh_y = 0, \tag{62}$$

$$h_t + (uh)_x + (vh)_y = 0, \tag{63}$$

and construct a fourth-order accurate invariant compact scheme for this PDE as well. The symmetry group associated

with this PDE is given in Ref. [52] as

$$X_1 = t^2 \frac{\partial}{\partial t} + x\,t\,\frac{\partial}{\partial x} + y\,t\,\frac{\partial}{\partial y} + (x - t\,u)\,\frac{\partial}{\partial u}$$
$$+ (y - t\,v)\,\frac{\partial}{\partial v} - 2ht\,\frac{\partial}{\partial h},$$

$$X_2 = x\,\frac{\partial}{\partial x} + y\,\frac{\partial}{\partial y} + u\,\frac{\partial}{\partial u} + v\,\frac{\partial}{\partial v} + 2h\,\frac{\partial}{\partial h},$$

$$X_3 = 2t\,\frac{\partial}{\partial t} + x\,\frac{\partial}{\partial x} + y\,\frac{\partial}{\partial y} - u\,\frac{\partial}{\partial u} - v\,\frac{\partial}{\partial v} - 2h\,\frac{\partial}{\partial h},$$

$$X_4 = y\,\frac{\partial}{\partial x} - x\,\frac{\partial}{\partial y} + v\,\frac{\partial}{\partial u} - u\,\frac{\partial}{\partial v},$$

$$X_5 = t\,\frac{\partial}{\partial x} + \frac{\partial}{\partial u},$$

$$X_6 = t\,\frac{\partial}{\partial y} + \frac{\partial}{\partial v},$$

$$X_7 = \frac{\partial}{\partial x},$$

$$X_8 = \frac{\partial}{\partial y},$$

$$X_9 = \frac{\partial}{\partial t}, \tag{64}$$

where the groups X_2 and X_3 can be combined to obtain a more general scaling group as follows:

$$X_g = \frac{3}{2}X_2 - \frac{1}{2}X_3 = -t\,\frac{\partial}{\partial t} + x\,\frac{\partial}{\partial x} + y\,\frac{\partial}{\partial y} + 2u\,\frac{\partial}{\partial u}$$
$$+ 2v\,\frac{\partial}{\partial v} + 4h\,\frac{\partial}{\partial h}.$$

Considering the subgroups X_1, X_7, X_8, X_9, and X_s, we can determine the relevant point transformations for this problem as

$$\tilde{t} = e^{-s_g}\frac{(t + s_9)}{\lambda},$$

$$\tilde{x} = e^{s_g}\frac{x + s_7}{\lambda},$$

$$\tilde{y} = e^{s_g}\frac{y + s_8}{\lambda},$$

$$\tilde{u} = e^{2s_g}[\lambda u + s_1(x + s_7)],$$

$$\tilde{v} = e^{2s_g}[\lambda v + s_1(y + s_8)],$$

$$\tilde{h} = e^{4s_g}[\lambda^2 h],$$

$$\tilde{u}_{\tilde{x}} = e^{s_g}[\lambda^2 u_x + s_1\lambda],$$

$$\tilde{u}_{\tilde{y}} = e^{s_g}[\lambda^2 u_y],$$

$$\tilde{v}_{\tilde{x}} = e^{s_g}[\lambda^2 v_x],$$

$$\tilde{v}_{\tilde{y}} = e^{s_g}[\lambda^2 v_y + s_1\lambda],$$

$$\tilde{h}_{\tilde{x}} = e^{3s_g}[\lambda^3 h_x],$$

$$\tilde{h}_{\tilde{y}} = e^{3s_g}[\lambda^3 h_y], \tag{65}$$

where $\lambda = 1 - s_1(t + s_9)$. The symmetry parameters s_7, s_8, and s_9 can be determined via normalization conditions $\tilde{x}^{(i,j,n)} = 0$, $\tilde{y}^{(i,j,n)} = 0$ and $\tilde{t}^{(i,j,n)} = 0$. And as for the symmetry parameter s_1, similar to the 2D viscous Burgers' equation case, we can select different definitions for each PDE in Eqs. (61)–(63). For instance, for these equations, we can respectively select the normalization conditions $\tilde{u}_{\tilde{x}}^{(i,j,n)} = 0$, $\tilde{v}_{\tilde{y}}^{(i,j,n)} = 0$ and $\tilde{u}_{\tilde{x}}^{(i,j,n)} + \tilde{v}_{\tilde{y}}^{(i,j,n)} = 0$, which correspond to

$$\widehat{s_1} = -u_x^{(i,j,n)},$$

$$\bar{s}_1 = -v_y^{(i,j,n)},$$

$$\ddot{s}_1 = -\frac{1}{2}\left(u_x^{(i,j,n)} + v_y^{(i,j,n)}\right),$$

where the symbols $\widehat{(\cdot)}$, $\bar{(\cdot)}$ and $\ddot{(\cdot)}$ represent transformations based on different definitions of symmetry parameter s_1 in Eq. (65). Based on these transformations, the final form of the fourth-order accurate invariant compact scheme for this problem can be found as

$$\widehat{u}^{(i,j,n+1)} = \widehat{u}^{(i,j,n)} - \widehat{\tau}\big[\widehat{v}^{(i,j,n)}\widehat{u}_{\widehat{y}}^{(i,j,n)} + g\widehat{h}_{\widehat{x}}^{(i,j,n)}\big],$$

$$\bar{v}^{(i,j,n+1)} = \bar{v}^{(i,j,n)} - \bar{\tau}\big[\bar{u}^{(i,j,n)}\bar{v}_{\bar{x}}^{(i,j,n)} + g\bar{h}_{\bar{y}}^{(i,j,n)}\big], \tag{66}$$

$$\ddot{h}^{(i,j,n+1)} = \ddot{h}^{(i,j,n)} - \ddot{\tau}\big[\ddot{u}^{(i,j,n)}\ddot{h}_{\ddot{x}}^{(i,j,n)} + \ddot{v}^{(i,j,n)}\ddot{h}_{\ddot{y}}^{(i,j,n)}\big].$$

Performance of these invariant compact schemes is evaluated in the following section.

IV. RESULTS

In this section, performance of the proposed invariant compact finite-difference schemes developed for the inviscid Burgers' equation, linear advection-diffusion equation (in one and two dimensions), and viscous Burgers' equation (in one and two dimensions) is evaluated. Results obtained from the invariant schemes are compared with the standard schemes for numerical accuracy.

We first evaluate the performance of the invariant compact scheme constructed for the inviscid Burgers' equation, Eq. (23), by comparing the results with the high-order

TABLE I. Root-mean-square error (RMSE) and L_∞ error associated with numerical solutions of IBE given in Fig. 1.

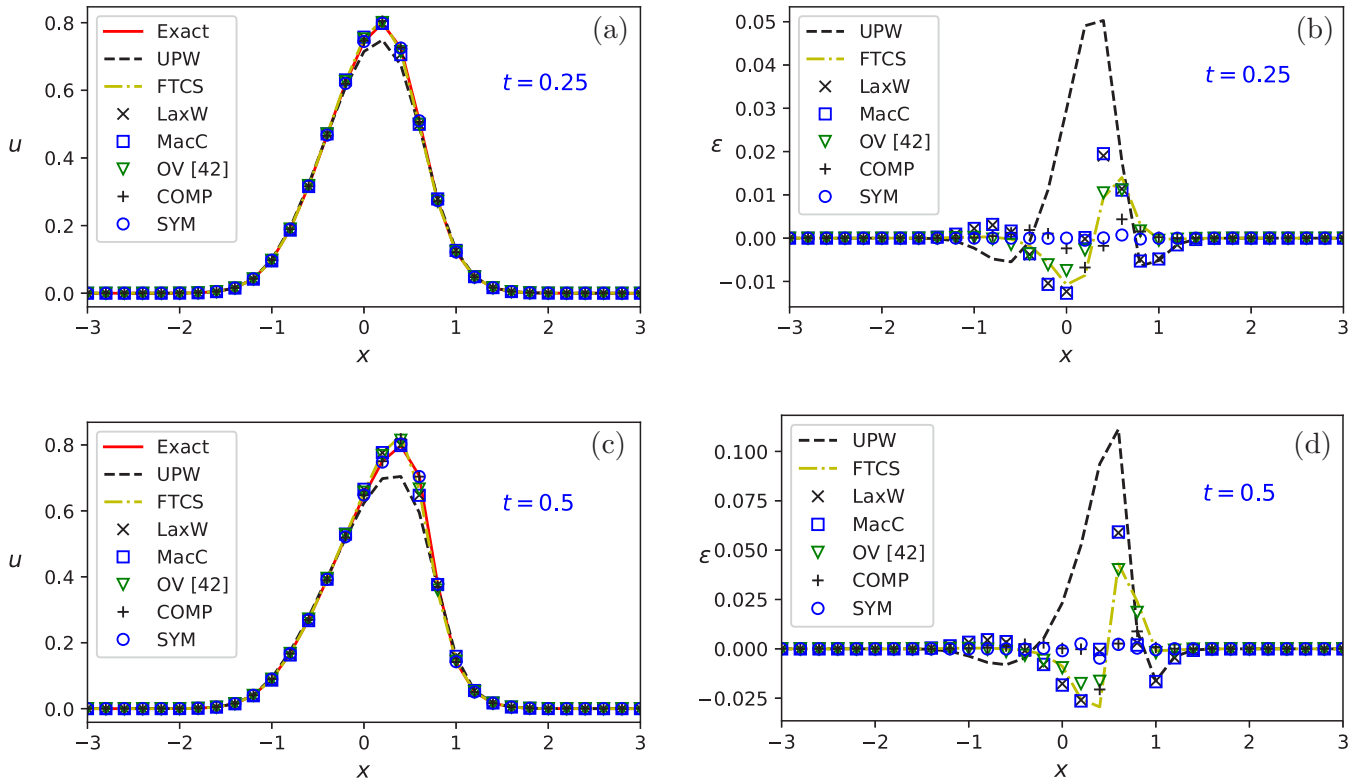| t	Error	UPW	FTCS	LaxW	MacC	OV [42]	COMP	SYM
0.25	L_∞	5.03×10^{-2}	1.40×10^{-2}	1.90×10^{-2}	1.95×10^{-2}	1.11×10^{-2}	6.78×10^{-3}	7.23×10^{-4}
	RMSE	1.44×10^{-2}	4.08×10^{-3}	5.18×10^{-3}	5.28×10^{-3}	3.37×10^{-3}	1.63×10^{-3}	1.61×10^{-4}
0.50	L_∞	1.11×10^{-1}	4.31×10^{-2}	5.88×10^{-2}	5.92×10^{-2}	4.01×10^{-2}	2.06×10^{-2}	4.69×10^{-3}
	RMSE	2.84×10^{-2}	1.14×10^{-2}	1.25×10^{-2}	1.26×10^{-2}	9.28×10^{-3}	4.12×10^{-3}	1.06×10^{-3}

FIG. 1. Inviscid Burgers' equation in one dimension. Comparison of velocity profiles, for $t = (0.25$ and $0.5)$, obtained from the analytical solution (Exact) and numerical solutions, based on standard forward in time and upwind (UPW) or central in space (FTCS) schemes, Lax-Wendroff scheme (LaxW), MacCormack scheme (MacC), the symmetry-preserving scheme proposed in Ozbenli and Vedula (OV [42]), standard compact scheme (COMP), and the proposed invariant compact scheme (SYM) is shown in the left plots (a), (c). Spatial distribution of numerical errors for these schemes is displayed in the right plots (b), (d). Parameter settings: $h = 0.2$, $\tau = 0.0208$, and $\sigma = 0.5$.

numerical solution obtained from the implicit relation

$$u(t, x) = \frac{1}{\sqrt{2\pi\sigma^2}} \exp\left\{-\frac{[x - u(t,x)t]^2}{2\sigma^2}\right\} \quad (67)$$

over the spatial domain $\Gamma(x)$, where $x \in [-3, 3]$. The initial and boundary conditions are also noted from this implicit solution.
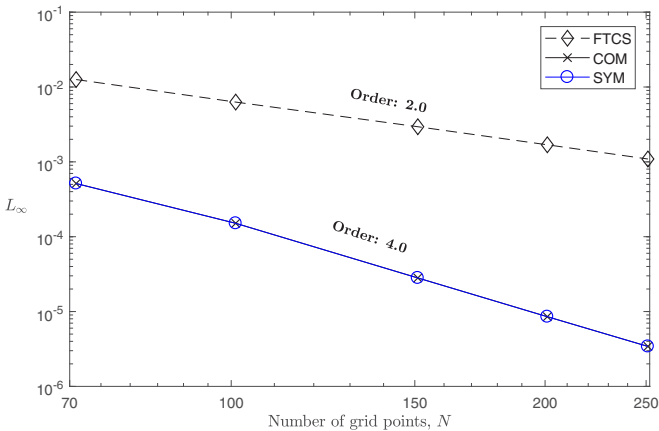

FIG. 2. Inviscid Burgers' equation. Comparison of L_∞ errors associated with various numerical schemes (FTCS, COM, SYM) as a function of number of grid points.

Snapshots of the propagating wave, for $t = 0.25$ and 0.5, that are obtained from the exact solution, the proposed invariant compact scheme (SYM), the standard fourth-order accurate compact scheme (COMP), and other selected schemes are shown in Figs. 1(a) and 1(c). The associated numerical errors of these schemes, which are estimated as $N_{\text{exact}} - N_{\text{numeric}}$, are also given in Figs. 1(b) and 1(d). It appears that the results obtained from the proposed invariant compact scheme (SYM) are significantly more accurate than those obtained from the standard schemes [based on upwind differencing (UPW), central differencing (FTCS), Lax-Wendroff (LaxW), and MacCormack (MacC) methods] and are slightly better than those obtained from the standard compact finite-difference scheme (COMP) and the symmetry-preserving scheme proposed by Ozbenli and Vedula (OV [42]). Further, the root-mean-square error (RMSE), estimated as $\sqrt{\sum(u_a - u_n)^2/N}$, and L_∞ error, estimated as $\max(|u_a - u_n|)$, of these numerical schemes, for the parameter settings presented in Fig. 1, are given in Table I. According to this error analysis, for $t = 0.25$, the L_∞ errors obtained from the proposed invariant compact scheme, the standard (noninvariant) compact scheme (COMP), and the standard scheme based on central differencing (FTCS) are 7.23×10^{-4}, 6.78×10^{-3}, and 1.04×10^{-2}, respectively, where other schemes have higher errors. Similarly, the RMSEs for these numerical schemes are measured as 1.61×10^{-4} (for SYM), 1.63×10^{-3} (for COMP), and 4.08×10^{-3} (for FTCS). A similar trend is observed in L_∞ and RMSEs for $t = 0.5$.
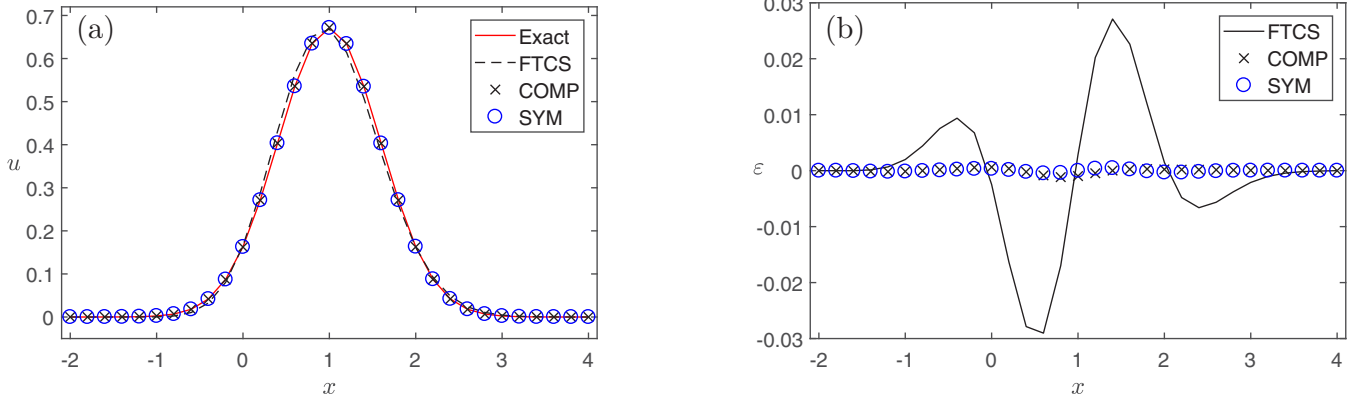
FIG. 3. Linear advection-diffusion equation in one dimension. Snapshots of wave profiles, for $t = 1.0$, obtained from the analytical solution (Exact), the classical forward in time central in space scheme (FTCS), the standard compact scheme (COMP), and the proposed invariant compact scheme (SYM) are displayed in (a). Spatial distribution of errors is displayed in (b). Parameter settings: $h = 0.2$, $\tau = 0.001$, $\nu = 1/60$.

Results indicate that the proposed invariant scheme (SYM) has significantly less error compared to the standard FTCS and compact schemes.

The variation of L_∞ errors (obtained from the standard FTCS scheme, standard compact finite-difference scheme, and the invariant scheme) with respect to the number of spatial grid points is demonstrated in Fig. 2. The proposed invariant scheme (SYM) appears to be two orders more accurate than the standard second-order FTCS scheme and is at the same order as the standard compact finite-difference scheme, which is known to be fourth-order accurate. Here we note that a sufficiently small time step is considered for this simulation as the fourth-order compact algorithms [given in Eqs. (5) and (6)] are considered only for the spatial derivatives.

Further, we evaluated the performance of the proposed method by developing a fourth-order accurate invariant compact finite-difference scheme for the 1D linear advection-diffusion equation given in Eq. (29). The analytical solution

$$u(t, x) = \frac{1}{\sqrt{4\pi (L^2 + \nu t)}} \exp\left[-\frac{(x - \alpha t)^2}{4 (L^2 + \nu t)}\right] \quad (68)$$

is considered over the spatial domain $\Gamma[-2, 4]$, where the initial and boundary conditions are obtained from this solution. Here L is the characteristic width of the kernel and assumed to be equal to 0.4 for all test cases. For this particular problem, evolution of the profile $u(t, x)$ (from a given Gaussian initial profile) obtained from the proposed invariant scheme (SYM), standard FTCS scheme, and compact finite-difference (COMP) scheme is depicted in Fig. 3(a). The spatial distribution of errors obtained from these numerical solutions is also shown in Fig. 3(b). The invariant compact scheme appears

to capture the wave propagation significantly better than the FTCS scheme and slightly better than the compact scheme. Additionally, L_∞ error and RMSE measures corresponding to the proposed invariant compact scheme, FTCS scheme and standard compact finite-difference scheme are presented in Table II. It appears that the invariant compact scheme is two orders of magnitude more accurate than the FTCS scheme and is one order of magnitude more accurate than the standard compact finite-difference scheme.

Further, Fig. 4 shows the variation of L_∞ errors associated to the invariant compact scheme, FTCS scheme, and standard noninvariant compact scheme with respect to the number of spatial grid points. The invariant scheme appears to be two orders more accurate than the standard second-order FTCS scheme. Moreover, although both the invariant and standard noninvariant compact schemes are fourth-order accurate, the invariant scheme appears to have slightly less numerical error.

In our next test case, we considered 1D viscous Burgers' equation and developed a fourth-order accurate invariant compact scheme that preserves the whole symmetry group
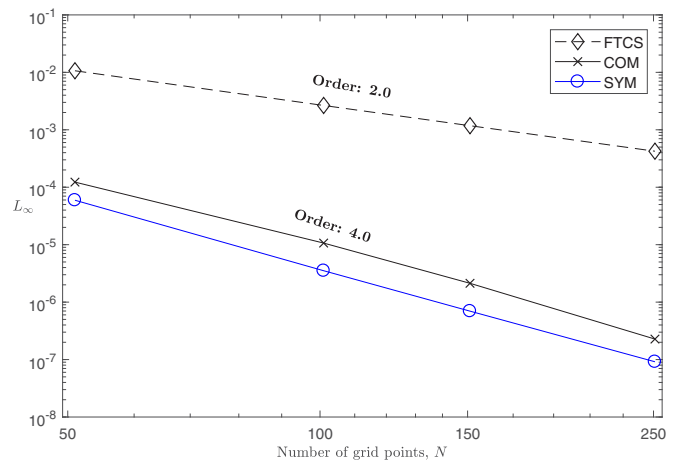
TABLE II. Root-mean-square error (RMSE) and L_∞ error associated with numerical solutions for 1D linear advection-diffusion equation.

Error	FTCS	COMP	SYM
L_∞	2.9×10^{-2}	1.2×10^{-3}	4.6×10^{-4}
RMSE	1.2×10^{-2}	3.7×10^{-4}	2.1×10^{-4}

FIG. 4. Linear advection-diffusion equation in one dimension. Comparison of L_∞ errors associated with various numerical schemes (FTCS, COM, and SYM) as a function of number of grid points.
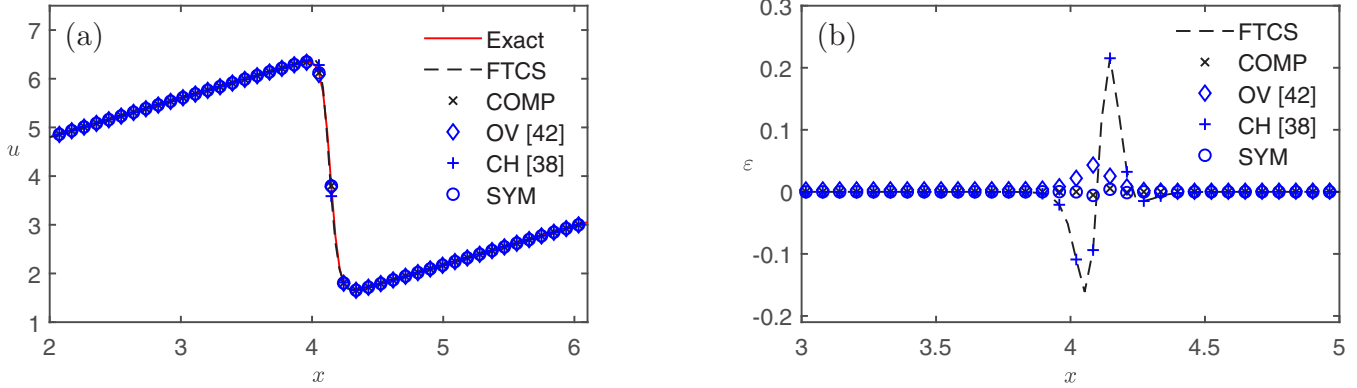
FIG. 5. Viscous Burgers' equation in one dimension. Snapshots of shock formation profiles, for $t = 0.25$, obtained from the analytical solution (Exact), the standard forward in time central in space scheme (FTCS), the standard compact scheme (COMP), the symmetry-preserving schemes presented in Chhay and Hamdouni (CH [38]) and Ozbenli and Vedula (OV [42]), and the proposed invariant compact scheme (SYM) are shown in (a). Spatial distribution of errors for these numerical schemes is displayed in (b). Parameter settings: $h = 0.01\pi$, $\tau = 10^{-6}$, $\nu = 1/12$.

associated with this PDE. The analytical solution

$$u(t, x) = -\frac{2\nu}{\phi} \frac{\partial \phi}{\partial x} + 4,$$

$$\phi = \exp\left[-\frac{(x - 4t)^2}{4\nu(t + 1)}\right] + \exp\left[-\frac{(x - 4t - 2\pi)^2}{4\nu(t + 1)}\right]$$

(69)

is considered over the spatial domain $\Gamma[0, 2\pi]$, where the initial and boundary conditions are determined from this solution.

Snapshots of the propagating shock, for $t = 0.25$, along with the spatial distribution of numerical errors, obtained from the proposed invariant compact scheme (SYM), the standard second-order FTCS scheme, the standard noninvariant compact scheme (COMP) and the symmetry-preserving schemes presented in Chhay and Hamdouni (CH [38]) and Ozbenli and Vedula (OV [42]) are shown in Fig. 5. Although a coarse grid with 201 nodes is used for this particular simulation, it appears that the proposed invariant scheme (SYM) performs well and captures the shock propagation better than the standard schemes, particularly near the shock front. Further, L_∞ error and RMSE analysis given in Table III also confirms that the invariant compact scheme (SYM) performs significantly better than the standard FTCS scheme and the symmetry-preserving scheme CH [38] and performs slightly better than the standard compact scheme (COMP) and the symmetry-preserving scheme OV [42]. Here we note that the symmetry-preserving scheme given in Chhay and Hamdouni (CH [38]) is constructed using second-order approximations for the spatial derivatives and hence are expected to perform with higher

errors compared to the compact schemes. It is important to remember that this scheme preserves the symmetries of the viscous Burgers' equation and has other advantages over the standard schemes. Similarly, the symmetry-preserving scheme given in Ozbenli and Vedula (OV [42]) has significant advantages over the standard schemes as well. Therefore, the reader is referred to the relevant references for further details on these schemes.

Further, the variation of L_∞ errors with respect to number of spatial grid points that is obtained from standard FTCS and compact (COM) schemes and the proposed invariant scheme (SYM) is shown in Fig. 6. As expected, the results obtained from the invariant scheme are indeed fourth-order accurate and are two orders more accurate than the standard FTCS scheme, which is known to be a second-order accurate scheme. Also, both the invariant scheme and the standard fourth-order compact scheme yield results of comparable order of accuracy with negligible differences.

Furthermore, as the proposed invariant compact scheme given in Eq. (37) preserves all the symmetry groups associated

TABLE III. Root-mean-square error (RMSE) and L_∞ error associated with numerical solutions of (1D) VBE given in Fig. 5.

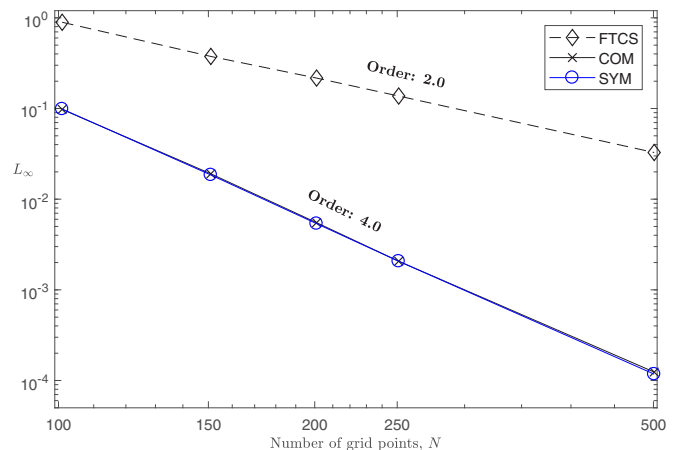| Error	FTCS	CH [38]	OV [42]	COMP	SYM
L_∞	2.2×10^{-1}	2.1×10^{-1}	4.3×10^{-2}	5.5×10^{-3}	5.7×10^{-3}
RMSE	2.5×10^{-2}	2.5×10^{-2}	6.0×10^{-3}	6.0×10^{-4}	5.9×10^{-4}

FIG. 6. Viscous Burgers' equation in one dimension. Comparison of L_∞ errors associated with various numerical schemes (FTCS, COM, and SYM) as a function of number of grid points.
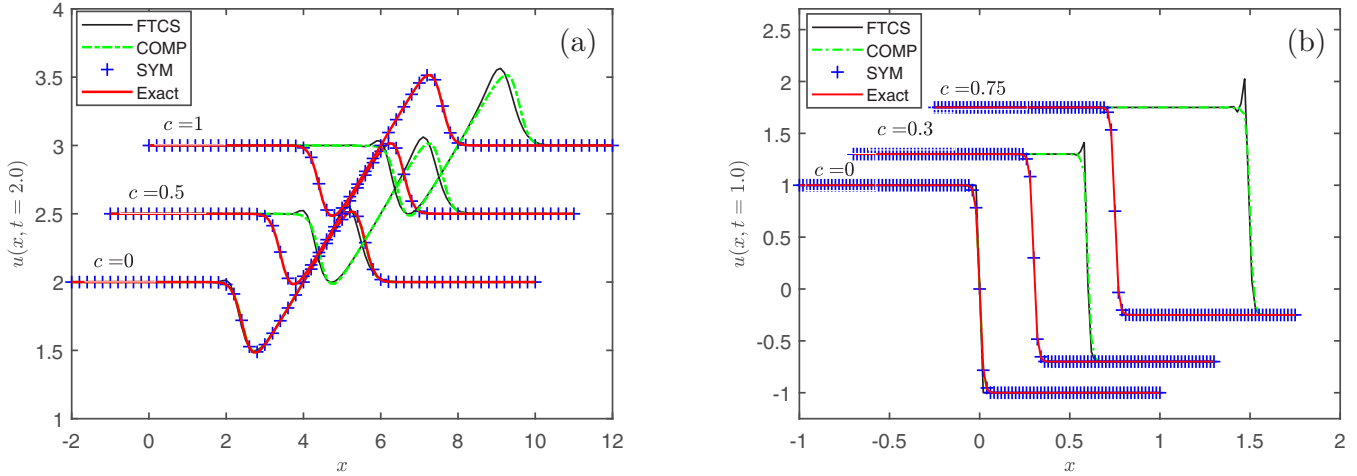
FIG. 7. Viscous Burgers' equation in one dimension. Snapshots of numerical solutions, obtained from the analytical solution (Exact), standard forward in time central in space scheme (FTCS), standard compact scheme (COMP), and proposed invariant compact scheme (SYM), evolving from various initial profiles for different values of the Galilean parameter c. (a) $h = 0.1$, $\tau = 0.0001$, $\nu = 0.05$, (b) $h = 0.02$, $\tau = 0.0005$, $\nu = 0.01$.

with the 1D viscous Burgers' equation, under transformations based on these symmetry groups, the invariant scheme is expected to perform significantly better than the standard schemes that ignore these symmetry groups. For instance, under a Galilean transformation of the form

$$\hat{x} = x + c\,t, \quad \hat{t} = t, \quad \hat{u} = u + c, \qquad (70)$$

the proposed invariant scheme (SYM) is likely to capture the evolution of the velocity profile significantly better than both the standard FTCS and compact schemes. This is expected as the invariant scheme preserves the Galilean transformation group X_2 given in Eq. (33), which is ignored in standard schemes. To test this particular advantage of the invariant scheme, we applied the Galilean transformation given in Eq. (70) to selected numerical schemes (i.e., FTCS, COMP, and SYM) and presented the results obtained from these schemes, based on two different initial profiles, in Fig. 7. Additionally, RMSEs and L_∞ errors associated with these numerical solutions are given in Tables IV and V. The details regarding the analytical solutions considered for the left and right plots in Fig. 7 can be found in Ref. [38]. Based on Fig. 7 and relevant error tables, it appears that when the Galilean parameter c is equal to zero, all the numerical schemes capture the evolution of the solution well, which is expected.

However, for the cases when the Galilean parameter c is nonzero, both the standard FTCS scheme and compact finite-difference scheme appear to overpredict the solution leading to a significant lag in the solution, particularly for large values of c. On the other hand, the invariant scheme, as it preserves the Galilean symmetry group, captures the evolution of the solution well even for nonzero values of the Galilean parameter c. In fact, in the case of a numerical precision considered in Tables IV and V, the results obtained from the invariant scheme for nonzero values of c are found to be identical to the results of the case where $c = 0$. The latter indicates that the Galilean invariance property of the viscous Burgers' equation is indeed preserved in the relevant difference equation. This property of symmetry preservation in numerical schemes can be particularly useful when differential equations associated to more complex symmetries are solved through difference equations.

As our fourth test case, we considered the 2D linear advection-diffusion equation and constructed two different fourth-order accurate invariant compact scheme (SYM-1 and SYM-2) for this PDE. The main difference between the constructed invariant schemes are that both are developed via selections of different moving frames, and the details of these selections are given in Sec. III D. The objective is to

TABLE IV. Variation of RMSE and L_∞ errors associated with numerical solutions presented in Fig. 7 (left) with respect to the Galilean parameter c.

c	Error	FTCS	COMP	SYM
0	L_∞	0.1157	0.0100	0.0120
	RMSE	0.0213	0.0023	0.0022
0.5	L_∞	0.5543	0.5131	0.0120
	RMSE	0.2424	0.2417	0.0022
1.0	L_∞	0.9033	0.9166	0.0120
	RMSE	0.3232	0.3206	0.0022

TABLE V. Variation of RMSE and L_∞ errors associated with numerical solutions presented in Fig. 7 (right) with respect to the Galilean parameter c.

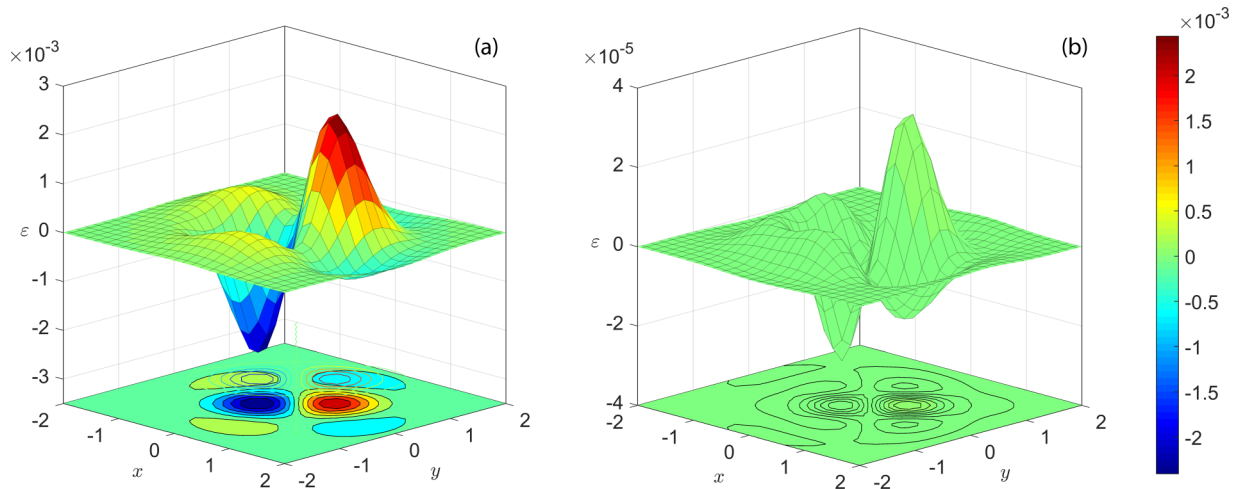| c	Error	FTCS	COMP	SYM
0	L_∞	0.2384	0.0269	0.0217
	RMSE	0.0339	0.0041	0.0034
0.3	L_∞	2.1117	2.0058	0.0217
	RMSE	0.7521	0.7451	0.0034
0.75	L_∞	2.2750	2.0118	0.0217
	RMSE	1.2066	1.2027	0.0034

FIG. 8. Linear advection-diffusion equation in two dimensions. Spatial distribution of numerical errors, for $t = 0.1$, obtained from the classical base scheme (a) and the proposed invariant scheme (b). Parameter settings: $h_x = 0.16$, $h_y = 0.16$, $\tau = 0.0001$, $\alpha = 1.0$, $\beta = 1.0$, $\nu = 1/60$.

investigate the effect of these selections on the accuracy of the resulting invariant schemes. The analytical solution

$$u(t, x, y) = \frac{1}{\sqrt{4\pi(L^2 + \nu t)}} \exp\left[-\frac{(x - \alpha t)^2 + (y - \beta t)^2}{4(L^2 + \nu t)}\right] \tag{71}$$

is used to evaluate the quality of results obtained from the invariant schemes SYM-1 and SYM-2.

Spatial distribution of numerical errors corresponding to the proposed invariant compact finite-difference scheme (SYM-2) and standard noninvariant FTCS scheme is given in Fig. 8. Based on this figure, it appears that the invariant scheme has significantly less numerical error compared to the standard noninvariant FTCS scheme in this case as well. This improvement in numerical accuracy is also verified by the error analysis given in Table VI, where both invariant schemes (SYM-1 and SYM-2) perform better than the standard schemes. L_∞ errors obtained from the invariant schemes SYM-1 and SYM-2, FTCS scheme and standard noninvariant compact scheme are noted as 3.4×10^{-5}, 3.3×10^{-5}, 2.4×10^{-3}, and 3.8×10^{-5}, respectively. It appears that the invariant schemes are at least two orders of magnitude more accurate than the standard FTCS scheme. RMSE measures of these numerical schemes also yield similar results, which are 3.3×10^{-6} and 3.1×10^{-6} for the invariant schemes SYM-1 and SYM-2, 2.7×10^{-4} for the FTCS scheme, and 3.4×10^{-6} for the noninvariant compact finite-difference scheme. The variation of L_∞ errors (obtained from the proposed invariant schemes, standard FTCS scheme, and noninvariant compact

scheme) with respect to the number of spatial grid points is presented in Fig. 9. As expected, both proposed invariant compact schemes constructed for the 2D linear advection-diffusion equation are indeed fourth-order accurate and perform significantly better than the second-order standard forward in time central in space finite-difference scheme (FTCS). Moreover, these invariant schemes also perform with slightly less error compared to the noninvariant compact scheme, which is known to be a fourth-order accurate scheme. Further, the invariant scheme SYM-2 appears to be slightly more accurate than the invariant scheme SYM-1, which indicates that the selection of moving frames could affect the accuracy of resulting invariant schemes. Although for this particular problem, the differences in the results obtained from the invariant schemes appear to be minor, in general the moving frames must be chosen carefully.
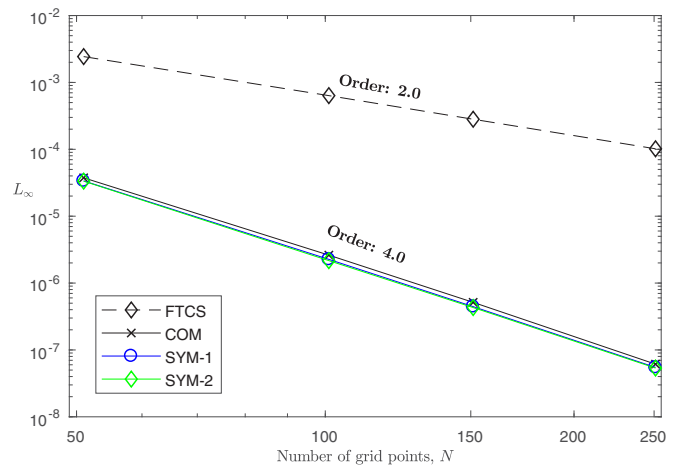

FIG. 9. Linear advection-diffusion equation in two dimensions. Comparison of L_∞ errors associated with various numerical schemes (FTCS, COM, SYM-1, and SYM-2) as a function of number of grid points.

TABLE VI. Root-mean-square error (RMSE) and L_∞ error associated with numerical solutions for 2D linear advection-diffusion equation.

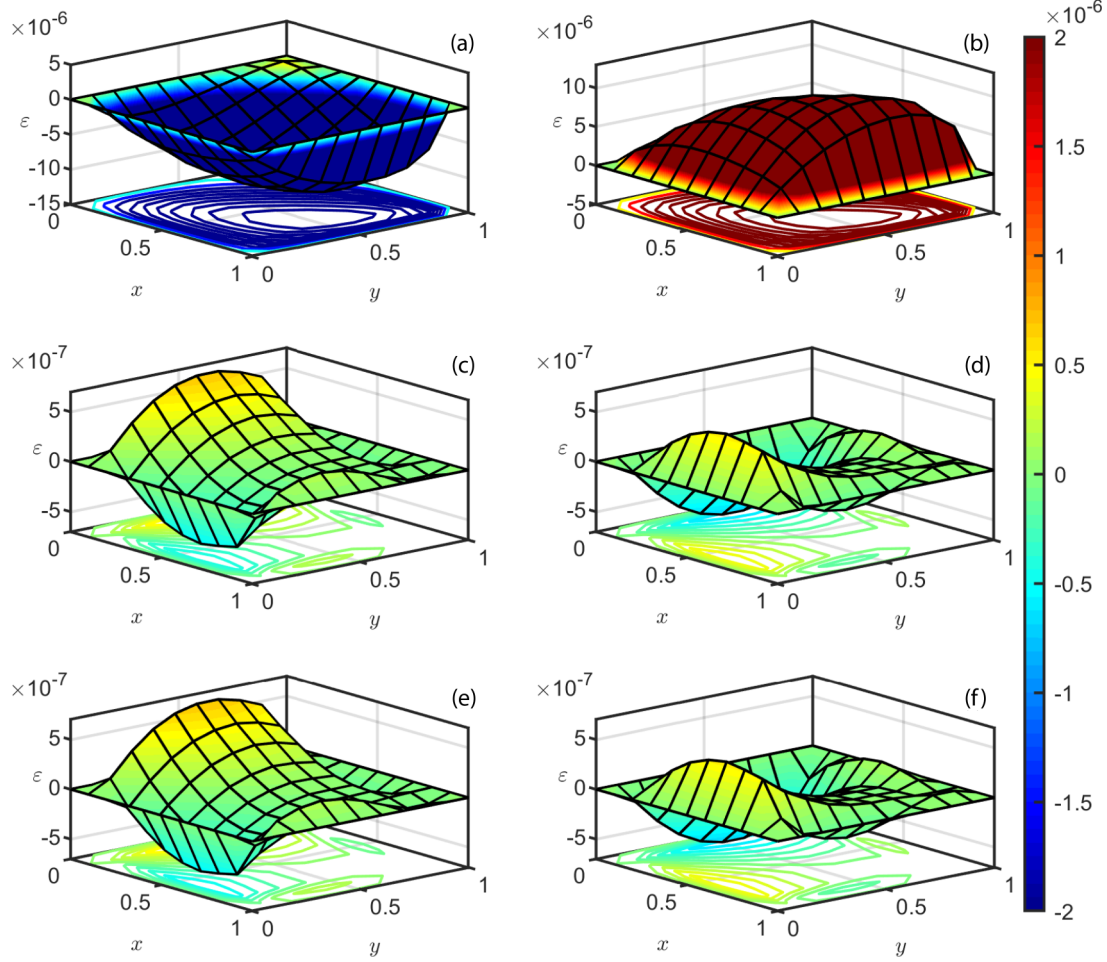| Error	FTCS	COMP	SYM-1	SYM-2
L_∞	2.4×10^{-3}	3.8×10^{-5}	3.4×10^{-5}	3.3×10^{-5}
RMSE	2.7×10^{-4}	3.4×10^{-6}	3.3×10^{-6}	3.1×10^{-6}

FIG. 10. Viscous Burgers' equation in two dimensions. Spatial distribution of numerical errors, based on velocity components u (left plots) and v (right plots), obtained from the standard FTCS scheme (a), (b), standard compact scheme (c), (d), and the proposed invariant scheme (e), (f) is shown. Parameter settings: $h_x = 0.1$, $h_y = 0.1$, $\tau = 0.00005$, and $\nu = 1/12$.

And as our fifth test problem, we considered the 2D viscous Burgers' equation and constructed a fourth-order accurate invariant compact scheme for this problem as well. The analytic solution considered for this case is

$$u(x, y, t) = \frac{3}{4} - \frac{1}{4\{1 + \exp[(-4x + 4y - t)/(32\nu)]\}},$$

$$v(x, y, t) = \frac{3}{4} + \frac{1}{4\{1 + \exp[(-4x + 4y - t)/(32\nu)]\}}, \quad (72)$$

where the initial and boundary conditions are noted from this solution. And based this analytical solution, numerical simulations are performed considering the spatial domain $\Gamma(x, y)$, where $x = [0, 1]$ and $y = [0, 1]$.

Spatial distribution of numerical errors, for $t = 0.25$, obtained from the standard forward in time central in space scheme (a), (b), standard fourth-order compact scheme (c), (d), and proposed invariant compact scheme (e), (f) is shown in Fig. 10, where the left and right plots represent measurements based on the velocity components u and v, respectively. L_∞ error and RMSE error measurements associated with these numerical schemes, for this particular simulation, are presented in Table VII. According to these results, it appears that the invariant scheme performs significantly better

than the standard FTCS scheme and is slightly more accurate than the noninvariant compact scheme.

In addition, Fig. 11 shows the variation of the L_∞ errors (obtained from the invariant compact scheme, standard noninvariant compact scheme, and the forward in time central in space scheme) with respect to number of grid points for sufficiently small time steps at $t = 0.25$. As expected the proposed invariant compact scheme is indeed fourth-order accurate. Comparison with the standard schemes shows that the invariant scheme is significantly more accurate than the FTCS scheme, which is known to be a second-order scheme and is also slightly more accurate than the standard fourth-order compact scheme.

TABLE VII. Root-mean-square error (RMSE) and L_∞ error associated with numerical solutions of (2D) VBE given in Fig. 10.

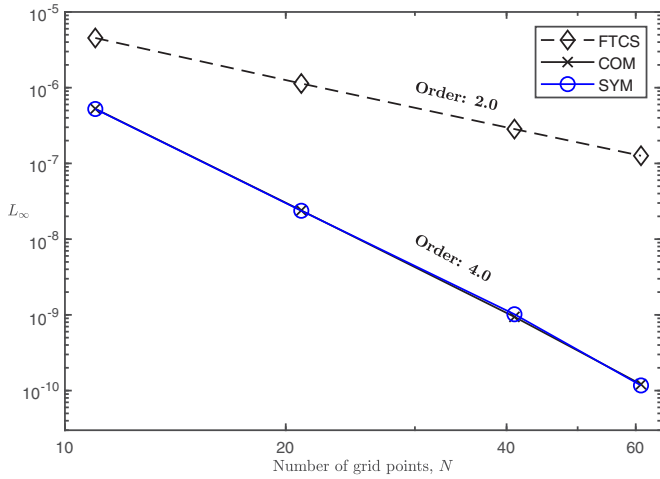|	Error	FTCS	COMP	SYM
u	L_∞	1.1×10^{-5}	7.0×10^{-7}	6.9×10^{-7}
	RMSE	5.5×10^{-6}	2.3×10^{-7}	2.3×10^{-7}
v	L_∞	1.1×10^{-5}	7.0×10^{-7}	7.0×10^{-7}
	RMSE	5.5×10^{-6}	2.3×10^{-7}	2.3×10^{-7}

FIG. 11. Viscous Burgers' equation in two dimensions. Comparison of L_∞ errors associated with various numerical schemes (FTCS, COM, SYM) as a function of number of grid points.

As our next test problem, we considered the 1D spherical Burgers' equation and constructed a fourth-order accurate invariant compact scheme, on a nonorthogonal mesh, that preserves the full symmetry groups associated with this PDE. The following analytical solution is used [51]:

$$u(t, x) = \frac{x}{t[1 + \ln(t)]}, \tag{73}$$

where the initial condition at $t = 1$ (to avoid division by zero) and the boundary conditions are noted from this equation.

Spatial distribution of numerical errors and associated root-mean-square and L_∞ error measures obtained from solutions based on the standard FTCS scheme, fourth-order compact scheme, and proposed invariant scheme, at $t = 1.3$, are given in Fig. 12 and Table VIII, respectively. The L_∞ errors associated with these numerical schemes are noted as
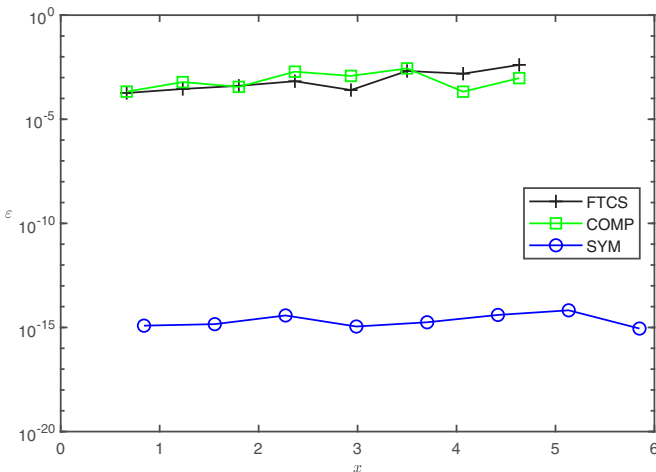

FIG. 12. Spherical Burgers' equation in one dimension. Spatial distribution of numerical errors, obtained from the standard FTCS scheme, standard fourth-order compact scheme (COMP), and the proposed invariant scheme (SYM) are shown. Parameter settings: $h = 0.57$ and $\tau = 6 \times 10^{-4}$.

TABLE VIII. Root-mean-square error (RMSE) and L_∞ error associated with numerical solutions for 1D spherical Burgers' equation.

Error	FTCS	COMP	SYM
L_∞	4.1×10^{-3}	2.8×10^{-3}	6.7×10^{-15}
RMSE	1.6×10^{-3}	1.2×10^{-3}	2.9×10^{-15}

5.9×10^{-3} for the standard FTCS scheme, 5.7×10^{-3} for the standard fourth-order accurate compact scheme (COMP), and 9.8×10^{-15} for the proposed invariant scheme (SYM). Similarly, the RMSEs for these schemes are found as 2.6×10^{-3} (FTCS), 5.7×10^{-3} (COMP) and 9.8×10^{-15} (SYM), respectively. Based on these results, it appears that the symmetry-preserving compact scheme is significantly more accurate (by about 11 orders of magnitude) than the standard FTCS and fourth-order accurate compact finite-difference schemes for this particular choice of analytical solution. Although it is reasonable to expect that preservation of symmetries in numerical schemes could lead to significant improvements in accuracy, we observe that such improvements are not always guaranteed. For instance, while our proposed symmetry based schemes for spherical Burgers' equation case showed considerable improvements in accuracy (by 11 orders of magnitude), a similar degree of improvement in accuracy was not observed in other cases (e.g., 2D viscous Burgers' equations, shallow water equations). We believe that there are important open research questions regarding the conditions under which we can definitively expect significant improvements in accuracy. Based on our experience, we believe that the selection of moving frames has a significant effect on the accuracy of our proposed symmetry-based numerical schemes. We observe that moving frames that result in removal of leading-order terms of the truncation error often result in considerable improvement in accuracy.

To further show the implementation of the proposed method to multidimensional problems, as our last test case, we considered the 2D, nonlinear shallow water equations and developed a fourth-order accurate symmetry-preserving compact scheme. Numerical simulations are performed over the domain $x, y \in [-5 \times 10^4, 5 \times 10^4]^2$ where solutions evolve from the following Gaussian initial profile:

$$u(t = 0, x, y) = 0, \quad v(t = 0, x, y) = 0,$$

$$h(t = 0, x, y) = A \exp\left[\frac{-(x - \mu_x)^2 - (y - \mu_y)^2}{2\sigma^2}\right].$$

For this particular simulation, we assume that walls are present at boundaries and hence use reflective boundary conditions where the flow in the direction of outward normal

TABLE IX. Root-mean-square error (RMSE) and L_∞ error associated with numerical solutions for 2D shallow water equations.

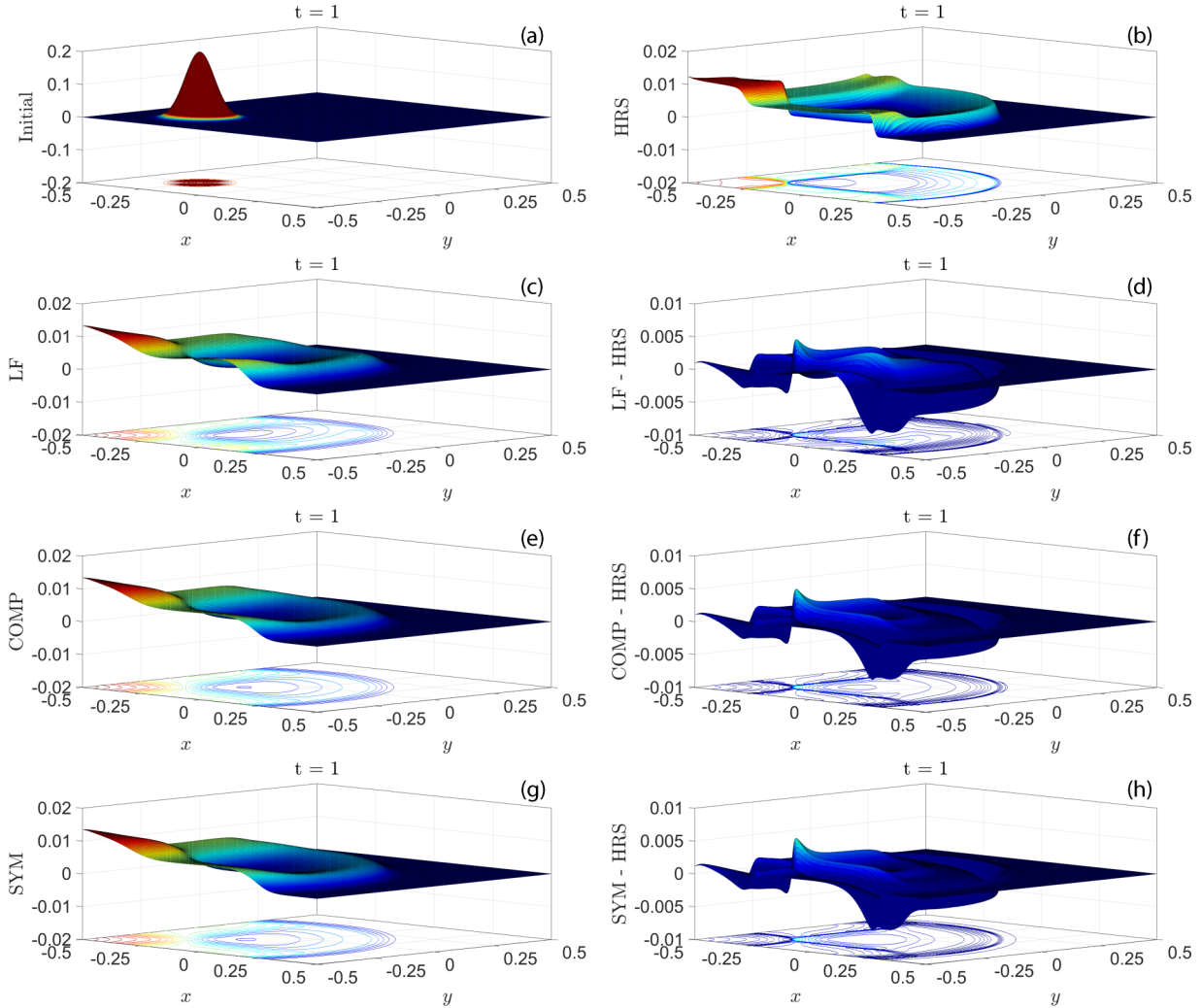| Error	LF	COMP	SYM
L_∞	7.0×10^{-3}	6.0×10^{-3}	5.8×10^{-3}
RMSE	1.6×10^{-3}	1.3×10^{-3}	1.2×10^{-3}

FIG. 13. Shallow water equations in two dimensions. Snapshots of numerical solutions at $t = 1$ along with spatial distribution of numerical errors, obtained from a high-resolution numerical solution (HRS), Lax-Friedrich scheme (LF), standard fourth-order accurate compact scheme (COMP), and proposed invariant scheme (SYM), evolving from a Gaussian initial profile (Initial) are shown. Parameter settings: $\Delta x = 0.005$, $\Delta t = 0.001$, $A = 0.2$, $\sigma^2 = 0.0005$, $\mu_x = -0.25$, $\mu_y = -0.25$.

is reflected back into the domain and the flow tangential to the boundaries remains the same. We compared the results with a high-resolution numerical solution to evaluate the performance of the proposed invariant compact numerical scheme. The snapshots of numerical solutions obtained from a high-resolution reference solution (HRS), Lax-Friedrichs scheme (LF), standard fourth-order accurate compact scheme (COMP), and the proposed invariant scheme (SYM) are given in Fig. 13. The spatial distribution of numerical errors, measured as $\varepsilon = h_{\text{numeric}} - h_{\text{HRS}}$, associated with these numerical solutions are also given in this figure. Further, L_∞ and RMSE measures shown in Table IX. Based on these results, it appears that the symmetry-preserving numerical scheme performs slightly better than the standard schemes in this case as well.

V. CONCLUSION

Compact finite-difference schemes are preferred over standard finite-difference schemes as these schemes enable high-order accuracy on stencils with comparably small number of grid points and have good, spectral-like resolution. In this paper, we presented a method, that is based on moving frames, for construction of invariant compact finite-difference schemes that preserve Lie symmetry groups of underlying partial differential equations. In this method, we first determine the extended symmetry groups of PDEs and then obtain point transformations based on these symmetry groups. These transformations are then applied to some (noninvariant) base compact finite-difference schemes such that all the system variables (i.e., independent and dependent variables) and derivatives of these compact schemes are transformed. We then determine the unknown symmetry parameters that exist in these symmetry-based point transformations by considering convenient moving frames that are obtained through Cartan's method of normalization. In most cases, such convenient moving frames not only result in significant improvement in numerical accuracy but also notably simplify the numerical representations of the resulting invariant schemes, and eventually make them easier to program. Performance of the proposed method was evaluated via construction of high-order

accurate invariant compact finite-difference schemes (built on simple three-point stencils) for some linear and nonlinear PDEs. Based on our evaluations, we concluded that symmetry preservation has the potential to significantly improve numerical accuracy of compact schemes, besides embedding important geometric properties of underlying PDEs.

As our first test case, we considered the inviscid Burgers' equation and constructed a high-order accurate invariant compact finite-difference scheme for this PDE. Although the order of accuracy of compact schemes can be arbitrarily set by considering suitable compact finite-difference algorithms, for this particular problem, we chose fourth-order accurate compact algorithms to approximate the spatial derivatives and constructed an invariant scheme based on these algorithms. In all the test problems, the temporal derivatives were handled through standard forward differencing. For this particular PDE, in order to improve the numerical accuracy from first to second order in time, the base scheme was modified using defect correction techniques. The results obtained from this fourth-order accurate invariant compact scheme were found to be slightly better than the results obtained from the standard compact scheme and were notably better than those of the standard FTCS scheme. For all the test cases, the computation times required to run a simulation with a numerical error of comparable order were found to be similar for both the proposed invariant scheme and standard compact scheme, and the differences were negligible.

As our next test problem, we considered the 1D linear advection-diffusion equation and developed a fourth-order accurate invariant compact scheme for this problem as well. For this particular problem, through the use of convenient moving frames (i.e., $\tilde{u}_{\tilde{x}\tilde{x}}^{(i,n)} = 0$), the numerical representation of the base scheme were reduced to a form of the linear advection equation, $\tilde{u}_{\tilde{t}}^{(i,n)} + \alpha \tilde{u}_{\tilde{x}}^{(i,n)} = 0$, in the transformed space. Similar to the previous problem, the quality of results obtained from this invariant compact scheme (in terms of numerical accuracy) was found to be better than that of the standard FTCS and compact schemes.

Next we constructed a fourth-order accurate invariant compact finite-difference scheme for the viscous Burgers' equation (which is of the form of a linear heat equation, $\tilde{u}_{\tilde{t}}^{(i,n)} = \nu \tilde{u}_{\tilde{x}\tilde{x}}^{(i,n)}$, in the transformed space for the normalization condition $\tilde{u}_{\tilde{x}}^{(i,n)} = 0$) that preserves all the symmetries of the Burgers' equation, and compared our results with the standard schemes. As expected, the proposed invariant compact scheme developed for this problem yielded more accurate results than standard schemes in this case as well. In particular, the performance of the proposed invariant scheme was significantly better than that of the standard schemes when a Galilean transformation is applied to these schemes (see Fig. 7 and Tables IV–V) to test how these schemes are affected by such transformations that are based on symmetries of the underlying differential equation. This is due to the fact that the invariant scheme preserves the Galilean symmetry group of the viscous Burgers' equation, whereas the standard schemes do not.

In order to demonstrate the implementation of the proposed method to a multidimensional problem, we considered the 2D linear advection-diffusion equation and constructed a couple of fourth-order accurate invariant compact schemes for this problem, where different moving frames are used in the construction of each invariant scheme to evaluate how this action effects the accuracy of the resulting schemes. For the first invariant scheme SYM-1, a normalization condition of the form $\tilde{u}_{\tilde{x}\tilde{x}}^{(i,j,n)} = 0$ is used to determine the projection group parameter s_1, whereas for the other invariant scheme (SYM-2), this particular parameter was determined using the normalization condition $\tilde{u}_{\tilde{x}\tilde{x}}^{(i,j,n)} + \tilde{u}_{\tilde{y}\tilde{y}}^{(i,j,n)} = 0$. Although both normalization conditions simplify the base compact scheme considered for this PDE notably, the latter condition reduces the base scheme to the form of a 2D linear advection equation, $\tilde{u}_{\tilde{t}}^{(i,j,n)} + \alpha \tilde{u}_{\tilde{x}}^{(i,j,n)} + \beta \tilde{u}_{\tilde{y}}^{(i,j,n)} = 0$, in the transformed space. As for the results obtained from these invariant schemes, SYM-2 appears to be slightly more accurate than SYM-1 where both schemes are notably more accurate than standard schemes. Although for this particular problem, selection of different moving frames in the construction of invariant schemes did not affect the accuracy of these schemes significantly, this may not be the case for other problems as there are usually infinitely many applicable moving frames, and not all of them will result in accurate invariant schemes.

In addition, to show the implementation of the proposed method to other nonlinear problems, we constructed fourth-order accurate invariant compact schemes for the 1D spherical Burgers' equation, 2D viscous Burgers' equation, and 2D shallow water equations as well. Similar to the previous problems, we considered convenient moving frames, which lead to considerable improvements in accuracy and simplifications in numerical representation, for these problems as well.

While the proposed method could be effectively used for construction of invariant compact finite-difference schemes with desired order of accuracy, there are a few issues that need to be addressed in more detail. Further research is required to understand how the performance of invariant compact schemes (constructed through the proposed method) is affected by the choice of subgroups (considered for preservation in the difference equation), choice of moving frames among infinite number of possibilities, and the nature of initial and boundary conditions and their compatibility with the selected subgroups. Based on our simulations, we observed that although it is possible to consider the whole symmetry group of a PDE for preservation in difference equations, this often leads to cumbersome numerical representations without notably enhancing numerical accuracy. For instance, in the case of the viscous Burgers' equation, the whole symmetry group of the PDE is preserved in the related difference equation. However, the advantages owing to the inclusion of the Galilean subgroup become significant only when the invariant scheme is actually transformed under a Galilean transformation as demonstrated in Fig. 7. Further, the choice of moving frames which are used to determine the unknown group parameters could affect the accuracy of resulting invariant schemes. To our knowledge, there is no systematic approach to select the best moving frame and one must consider all the pros and cons of a particular moving frame before making a selection. Based on our observations, we found that a moving frame that removes the leading-order terms from truncation error of a difference equation is usually a good choice as such

a moving frame also simplifies the base scheme (in the transformed space) and makes it easier to program. Moreover, the performance of the constructed invariant schemes might be affected by the chosen initial and boundary conditions, especially if these conditions are not compatible with the chosen subgroups. This might be due to the fact that some of the limitations of base difference equations carry over to the constructed invariant schemes. For instance, for cases where discontinuities develop in solutions, the performance of the constructed invariant schemes will undoubtedly depend on the chosen base numerical schemes. This obstacle could be avoided by selecting base schemes that are better suited to handle such discontinuities.

ACKNOWLEDGMENT

[1] R. S. Hirsh, J. Comput. Phys. **19**, 90 (1975).

[2] S. K. Lele, J. Comput. Phys. **103**, 16 (1992).

[3] M. Ciment and S. H. Leventhal, Math. Comput. **29**, 985 (1975).

[4] K. Mahesh, J. Comput. Phys. **145**, 332 (1998).

[5] W. Dai and R. Nassar, Num. Methods Partial Diff. Eq. **16**, 441 (2000).

[6] S. E. Sherer and J. N. Scott, J. Comput. Phys. **210**, 459 (2005).

[7] R. K. Shukla, M. Tatineni, and X. Zhong, J. Comput. Phys. **224**, 1064 (2007).

[8] D. P. Rizzetta, M. R. Visbal, and P. E. Morgan, Prog. Aerosp. Sci. **44**, 397 (2008).

[9] M. Cui, J. Comput. Phys. **228**, 7792 (2009).

[10] A. Shah, L. Yuan, and A. Khan, Appl. Math. Comput. **215**, 3201 (2010).

[11] G. Zhong and J. E. Marsden, Phys. Lett. A **133**, 134 (1988).

[12] H. Yoshida, Phys. Lett. A **150**, 262 (1990).

[13] R. I. McLachlan, Phys. Rev. Lett. **71**, 3043 (1993).

[14] M. Calvo and E. Hairer, Appl. Num. Math. **18**, 95 (1995).

[15] A. L. Islas, D. A. Karpeev, and C. M. Schober, J. Comput. Phys. **173**, 116 (2001).

[16] E. Hairer, C. Lubich, and G. Wanner, *Geometric Numerical Integration: Structure-Preserving Algorithms for Ordinary Differential Equations*, Springer Series in Computational Mathematics Vol. 31 (Springer-Verlag, Berlin, Heidelberg, 2006).

[17] S. D. Webb, J. Comput. Phys. **270**, 570 (2014).

[18] E. Gagarina, V. R. Ambati, S. Nurijanyan, J. J. van der Vegt, and O. Bokhove, J. Comput. Phys. **306**, 370 (2016).

[19] N. N. Yanenko and Y. I. Shokin, Amer. Math. Soc. Transl. **104**, 259 (1976).

[20] V. A. Dorodnitsyn, Intl. J. Mod. Phys. C **05**, 723 (1994).

[21] M. I. Bakirova, V. A. Dorodnitsyn, and R. V. Kozlov, J. Phys. A: Math. Gen. **30**, 8139 (1997).

[22] V. A. Dorodnitsyn and P. Winternitz, Nonlin. Dyn. **22**, 49 (2000).

[23] V. A. Dorodnitsyn and R. Kozlov, J. Nonlin. Math. Phys. **10**, 16 (2003).

[24] V. A. Dorodnitsyn, *Applications of Lie Groups to Difference Equations* (CRC Press, New York, 2010).

[25] V. A. Dorodnitsyn, R. Kozlov, S. V. Meleshko, and P. Winternitz, J. Phys. A: Math. Theor. **51**, 205202 (2018).

[26] C. J. Budd and G. J. Collins, *Numerical Analysis*, Vol. 380 (Addison Wesley Longman Ltd, Boston, MA, 1997).

[27] P. E. Hydon, Eur. J. Appl. Math. **11**, 515 (2000).

[28] C. Budd and V. Dorodnitsyn, J. Phys. A: Math. Gen. **34**, 10387 (2001).

[29] D. Levi and P. Winternitz, J. Phys. A: Math. Gen. **39**, R1 (2005).

[30] A. Bourlioux, C. Cyr-Gagnon, and P. Winternitz, J. Phys. A: Math. Gen. **39**, 6877 (2006).

[31] E. Hoarau and C. David, arXiv:math/0611895v1.

[32] D. Levi, L. Martina, and P. Winternitz, J. Phys. A: Math. Theor. **48**, 025204 (2014).

[33] M. Fels and P. J. Olver, Acta Appl. Math. **51**, 161 (1998).

[34] M. Fels and P. J. Olver, Acta Appl. Math. **55**, 127 (1999).

[35] P. Kim, *Invariantization of Numerical Schemes for Differential Equations Using Moving Frames* (University of Minnesota Press, Minneapolis, 2006).

[36] P. Kim, BIT Numer. Math. **47**, 525 (2007).

[37] P. Kim, Physica D **237**, 243 (2008).

[38] M. Chhay and A. Hamdouni, Symmetry **2**, 868 (2010).

[39] M. Chhay, E. Hoarau, A. Hamdouni, and P. Sagaut, J. Comput. Phys. **230**, 2174 (2011).

[40] A. Bihlo and F. Valiquette, in *Symmetries and Integrability of Difference Equations*, edited by D. Levi, R. Rebelo, and P. Winternitz, CRM Series in Mathematical Physics (Springer, Cham, 2017), pp. 261–324.

[41] E. Ozbenli and P. Vedula, Phys. Rev. E **96**, 063304 (2017).

[42] E. Ozbenli and P. Vedula, J. Comput. Phys. **349**, 376 (2017).

[43] E. Ozbenli, Ph.D. thesis, University of Oklahoma (2018).

[44] É. Cartan, *Exposés de Géometrié*, Vol. 5 (Hermann et Cie, Editeurs, 1935).

[45] N. H. Ibragimov, *CRC Handbook of Lie Group Analysis of Differential Equations* (CRC Press, New York, 1995), Vol. 3.

[46] B. Cantwell, *Introduction to Symmetry Analysis*, Cambridge Texts in Applied Mathematics Vol. 29 (Cambridge University Press, New York, 2002).

[47] L. V. Ovsiannikov, *Group Analysis of Differential Equations* (Academic Press, New York, 1982).

[48] K. T. Vu, G. F. Jefferson, and J. Carminati, Comput. Phys. Commun. **183**, 1044 (2012).

[49] M. Oberlack, Flow, Turbul. Combust. **62**, 111 (1999).

[50] C.-W. Shu and S. Osher, J. Comput. Phys. **77**, 439 (1988).

[51] R. Rebelo and F. Valiquette, J. Diff. Eq. Appl. **19**, 738 (2013).

[52] A. Chesnokov, Eur. J. Appl. Math. **20**, 461 (2009).